[redacted]

WT-1364

This document consists of 56 pages

No. 184 of 225 copies, Series A

Operation REDWING

[redacted]

PACIFIC PROVING GROUNDS

May - July 1956

Adjunct to Project 30.2

GROUND-MOTION STUDIES

Issuance Date: June 25, 1958

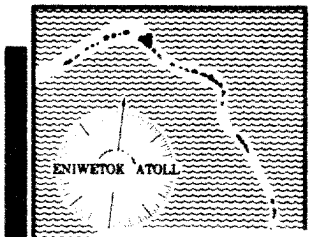

[redacted]

JOINT TASK FORCE SEVEN

[redacted]

AEC Technical Information Service Extension
Oak Ridge, Tennessee

Report to the Scientific Director

GROUND-MOTION STUDIES

By
William R. Perret

Sandia Corporation
Albuquerque, New Mexico
April 1957

[redacted]

ABSTRACT

Instrument container tests, adjuncts to Project 30.2 of Operation Redwing, yielded data relevant to ground motion at high overpressure regions for surface burst (LaCrosse shot) and tower burst (Blackfoot shot). Peak accelerations were observed at four stations ranging between 425- and 52-psi incident overpressures. These data, analyzed as functions of overpressure, showed a power-law relationship similar to that found for data from Mike shot of Operation Ivy:

$$A = K\Delta p^{1.2}$$

where A is peak acceleration, Δp is peak incident overpressure, and K is a coefficient which, for Redwing data, is about three times the value for Ivy data.

Velocity and displacement data were derived from the acceleration-time curves. However, data beyond peak accelerations were considered representative of ground motion in only three cases. This limits useful ground displacement information from these data to the 50- to 60-psi overpressure region.

Acceleration spectra were derived and are included for systems having zero damping and 3 and 10 percent critical damping. An appendix includes acceleration spectra from several sets of ground-motion data from Operations Ivy and Upshot-Knothole.

CONTENTS

CONTENTS (cont)

FIGURES

CHAPTER 1

INTRODUCTION

1.1 PURPOSE

Development and field tests of improved recording or telemetering techniques and equipment are ever-present phases of the work of the Sandia Corporation Field Test Organization. One such study was undertaken during Operation Redwing to determine the shock-loading parameters for which small buried recording or telemetering units must be designed to permit operation in regions of high incident air-shock overpressures. This study produced, in addition to information for instrument design, some basic data on ground motion which extended previous knowledge into regions of overpressure not previously documented. This report presents and evaluates the new ground-motion data.

1.2 BACKGROUND

A considerable fund of knowledge of motion induced in the ground by incidence of air shock has been developed within certain restrictions. Information concerning such ground motion derived from nuclear bursts is limited to a few programs involving air bursts in Nevada (References 1, 2, 3, and 4) equivalent to tens of kilotons of TNT energy and one surface burst at Eniwetok (Reference 5) equivalent to megatons of TNT energy. These data have, in general, derived from observation of acceleration at various depths, principally less than 20 feet, but in a few cases as deep as 50 feet. Observations have been limited to regions of incident overpressures of the order of 60 psi or less, although a few data for higher overpressures exist (References 1 and 4).

Some ground-motion data have been transformed by integration from acceleration-time information to velocity- and displacement-time information, particularly in data from Operations Ivy (Reference 5) and Upshot-Knothole (Reference 4). More recently, acceleration frequency spectra have been derived for the data just mentioned. Acceleration-frequency spectra indicate the maximum accelerations to which a simple mechanical oscillator of the specified natural frequency would be driven by an external force having the recorded acceleration-time parameter. Frequency spectra from Ivy and Upshot-Knothole data have previously been given only limited circulation and, therefore, are included as an appendix to this report to increase their availability.

different soils: (1) dry silt and sand of the Frenchman Flat area in Nevada and (2) saturated loose or cemented coral sand at Eniwetok atoll. Data obtained from the mock-up telemetering package tests made on Operation Redwing extend the range of incident overpressure for Eniwetok ground-motion studies from a maximum of about 40 psi for Operation Ivy to about 400 psi.

CHAPTER 2

THE EXPERIMENT

2.1 DESIGN OF THE EXPERIMENT

The primary purpose of the telemeter package test was to observe accelerations and displacements to which a container of appropriate dimensions would be subject when placed in the ground at shallow depths and subjected to relatively high overpressure air-shock-induced ground loading. The first phase of this test was made an adjunct to Project 30.2 for LaCrosse shot of Operation Redwing. Five mock-up canisters without telemeter equipment, but containing accelerometers and inertial scratch gages, were placed in the ground. Four were situated adjacent to Stations 3021, 3022, 3023, and 3024, and the fifth was approximately midway between Stations 3021 and 3022 (Figure 2.1). Code designations, ground ranges, and other pertinent data for these canisters are included in Table 2.1.

The second phase of the test, which was made in conjunction with Blackfoot shot, comprised two mock-up canisters placed in the ground near the instrumentation shelter, Station 3020 (Figure 2.1). Pertinent data for this instrumentation are included in Table 2.1.

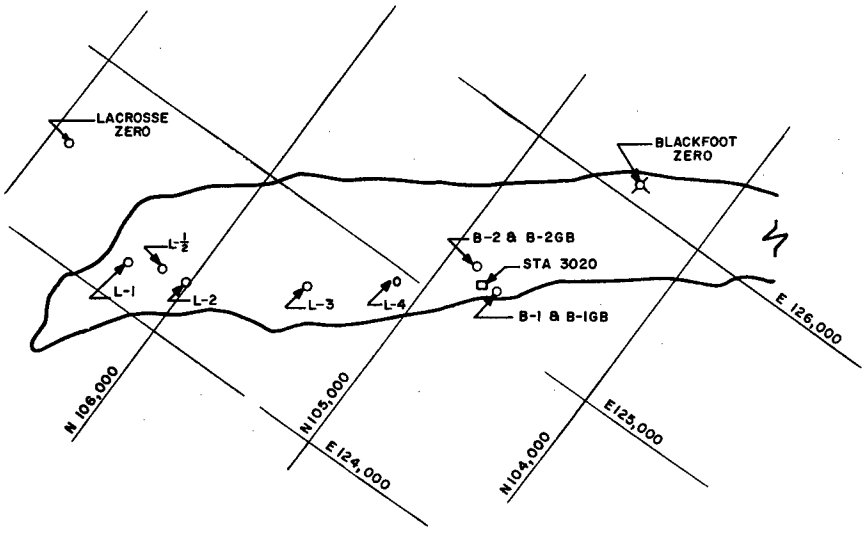

Figure 2.1 Yvonne site plan, LaCrosse and Blackfoot shots.

TABLE 2.1 GROUND-MOTION DATA

Canister	Accelerometer	Ground Range (ft)	Peak Overpressure (psi)	Peak Acceleration (g)	Station Adjacent
L-1	L-1AV	690	425	216	3021
L-1/2	L-1/2AV	818	200 (est)	81	--
L-2	L-2AV	920	154	67.4	3022
	L-2AR	920	154	36.2	3022
	L-2AT	920	154	10	3022
L-3	L-3AV	1400	55	17.1	3023
L-4	L-4AV	1825	No Record		3024
B-1	B-1AV	870	52	34.6	3020
B-2	B-2AV	870	72	52	3020

L indicates LaCrosse shot station
B indicates Blackfoot shot station
Numbers correspond to nearest Project 30.2 stations
1/2 refers to instrument midway between Stations 3021 and 3022
A refers to accelerometer
V, R, and T refer to vertical, radial, and tangential components

2.2 INSTRUMENTATION

Each canister included an accelerometer installed to respond to vertical motion; i.e., motion parallel to the axis of the cylindrical canister. In addition, canisters used in the first phase included an inertial mass and scratch gage for indicating maximum vertical displacement. One of the canisters included two additional accelerometers mounted to respond to radial and tangential[1] motion.

Mock-up canisters were made of 3-foot lengths of 10-1/2-inch-diameter seamless steel tubing. Plates of 1/4-inch steel were welded over one end of each tube, and the other ends were closed by 1/4-inch steel plates bolted to flanges welded to the tubing. Gaskets sealed the joints between cover plates and flanges. Figure 2.2 illustrates the approximate construction and position of instruments in the canisters. Circular plates of 1-inch-thick steel for mounting accelerometers were bolted across the midsection of the canisters parallel to the ends. Accelerometers responding to axial motion of the canisters were attached directly to the central plates. A machined block was attached to the central plate of Canister L-2 to permit installation of additional accelerometers responding to motion in two orthogonal directions normal to the canister axis.

[1]Ground-motion components refer to a cylindrical coordinate system with origin at ground zero and radial and tangential components parallel to the horizontal ground surface.

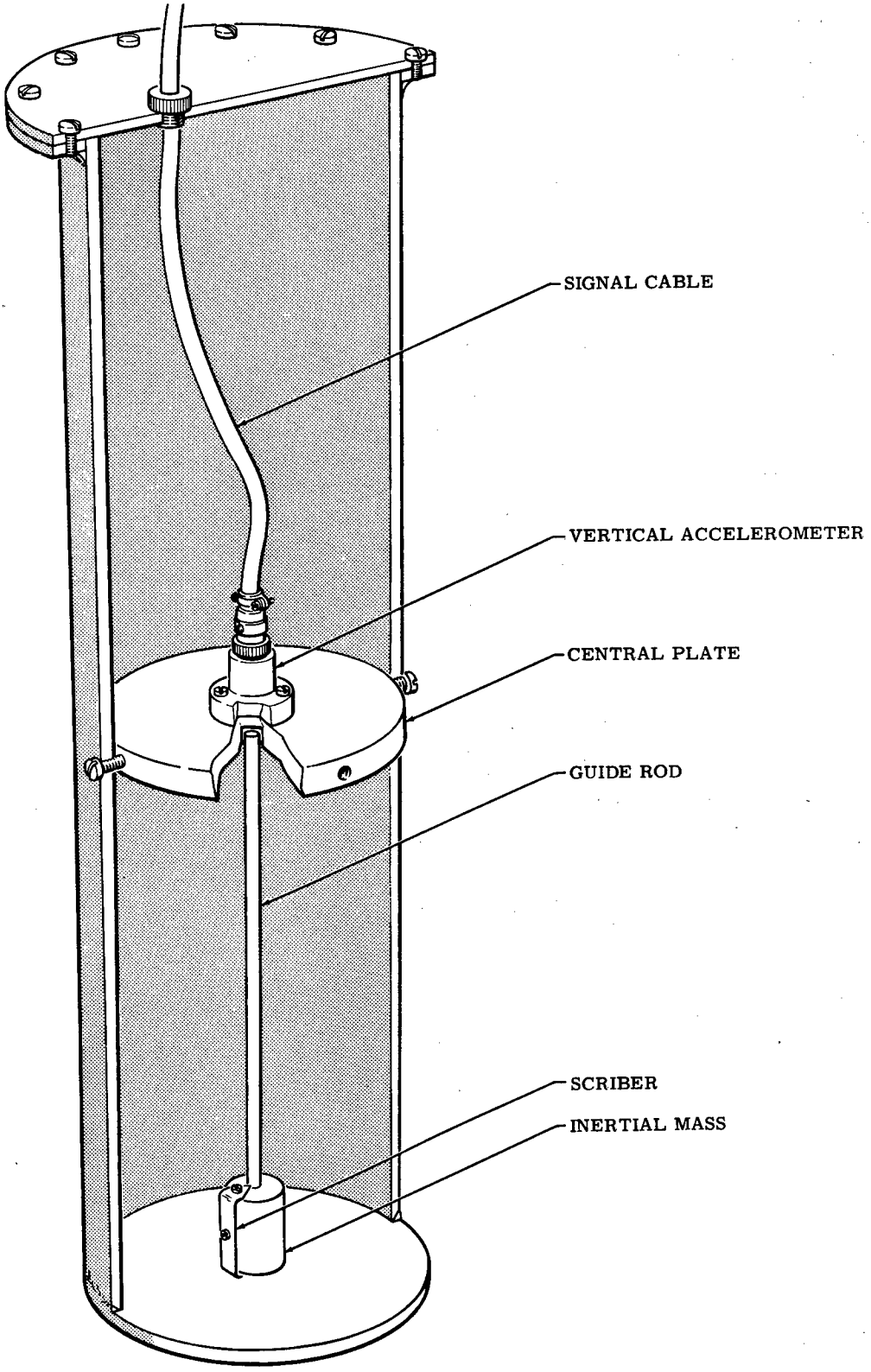

Figure 2.2 Mock-up canister.

Inertial masses for axial displacement scratch gages used in the first phase of this test were 2-inch-diameter brass blocks, 3 inches long. These blocks were drilled axially to slide freely on 5/8-inch-diameter aluminum rods. The rods were mounted on the canister axes below the central plates. They were screwed rigidly into the bottom plates and extended about 1/4 inch into oversize counterbores in the underside of the central plates. Upper ends of the rods were not supported by the plates, but were restricted to very small lateral or axial motion by them. Spring-steel scribers attached to the inertial masses recorded motion by scratching the aluminum rods, which were coated with dykum blue to aid legibility.

Accelerometers were of the variable-reluctance type manufactured by Wiancko Engineering Company. End instruments were connected through buried cables to a 3-kc carrier-amplifier, the rectified output of which was recorded on a multichannel magnetic tape recorder. Individual channels were played back and reproduced as photographic records of acceleration versus time at scales suitable for analysis.

Canisters, with one exception, were buried in the vicinity of ground baffle stations instrumented to measure incident air overpressure as a function of time. Canister L-1/2, containing Accelerometer L-1/2AV, was placed between Stations 3021 and 3022, where no overpressure measurement was made. Each canister was buried so that its top was about 1 foot below ground level, and its axis was vertical. The bottoms of most canisters, 4 feet below the ground surface, were above the water table. However, Canisters L-1 and L-1/2, those closest to LaCrosse shot ground zero, were in an area of relatively low elevation, with the result that their lower ends were submerged at high tide and were in wet sand at low tide.

CHAPTER 3

ANALYSIS OF RESULTS

3.1 RESULTS

Acceleration records were obtained from four of the five mock-up canisters installed for LaCrosse shot and from both canisters installed for Blackfoot shot. The record from Accelerometer L-4AV, adjacent to Station 3024 on LaCrosse shot, was lost because of recorder malfunction. Data from Accelerometer L-1AV were limited, by circuit failure, to a period of 10 milliseconds after shock arrival. Canister damage under high air-shock loading at the three stations closest to LaCrosse ground zero limited usefulness of the acceleration records. Displacement scratch-gage records were legible for four canisters, but several were not dependable because guide rods were bent by canister damage.

3.2 GROSS EFFECTS

Canisters L-1/2 and L-2, two of the five canisters installed for LaCrosse shot, sustained gross damage consisting of dished-in bottom plates (Figure 3.1) and bent scratch-gage guide rods (Figures 3.2 and 3.3). Canister L-1, closest to ground zero, was not recovered, but it is presumed to have been damaged as badly as L-1/2. The lower ends of Canisters L-1/2 and L-2 were in either saturated or moist sand, which was considerably more resistant to rapid penetration of rigid objects than the overlying dry loose sand.

The result of this situation, coupled with high-incident overpressure, seems to have been that the more rigid walls of the canisters transmitted the very high loading impressed on the top more rapidly and at higher strength than the corresponding load was transmitted through the dry sand. Passive resistance of the underlying wet sand loaded the bottom plates sufficiently to bend them inward permanently and probably produced considerably greater transient bending. The bottom of Canister L-1/2 was dished permanently about 1/2 inch. The bottom of Canister L-2, probably in drier sand, was bent only about 1/8 inch inward. Dishing of bottom plates forced the guide rods upward against the central plates, with consequent perturbation of accelerometer response and serious deformation of the rods. Bent guide rods (Figures 3.2 and 3.3) restricted movement of the inertial masses and made some scratch records questionable. Scratch records are discernible in the photographs.

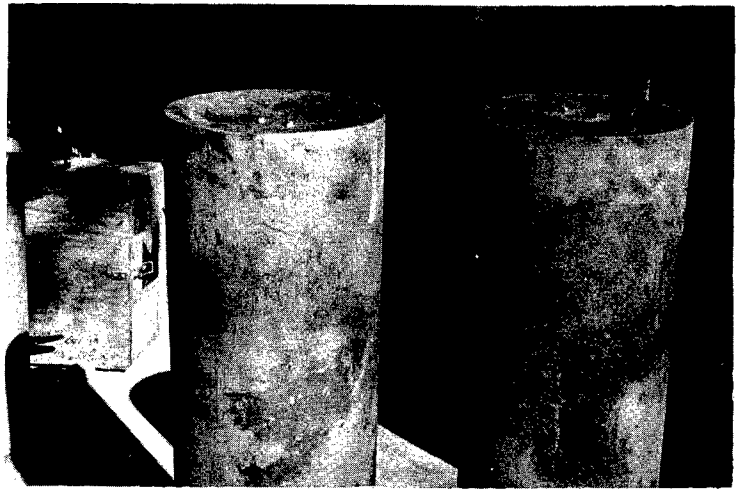

Figure 3.1 Bottoms of Canisters L-1/2 and L-2, post shot.

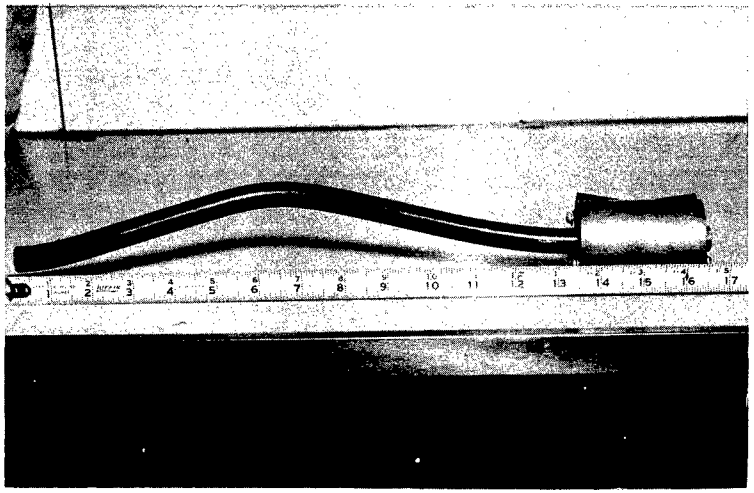

Figure 3.2 Scratch-gage guide rod and mass, Canister L-1/2.

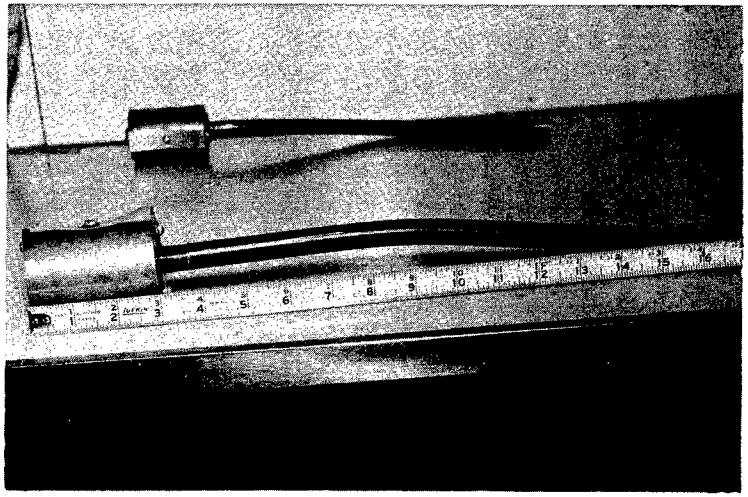

Figure 3.3 Scratch-gage guide rod and mass, Canister L-2 (foreground) and L-1/2 guide rod (background).

The other canisters, L-3 for LaCrosse shot and B-1 and B-2 for Blackfoot shot, show no damage or serious perturbation in acceleration records.

Records from canisters subjected to damaging loads indicate motion in which effects of guide-rod impact thoroughly mask ground motion after an interval of from 2 to 5 milliseconds following shock arrival. The consequence of gross damage effects is that only very early recorded peak accelerations can be interpreted as representing ground motion with reasonable precision.

3.3 ACCELERATION-OVERPRESSURE RELATIONSHIP

Peak vertical accelerations produced in the ground by air shock have, in several cases, been shown to bear a power-law relation to the peak incident overpressure (References 3 and 5). Initial peak vertical accelerations from the mock-up canisters which have been considered representative of initial ground motion were plotted on logarithmic scales as functions of peak overpressures (Figure 3.4). Data from Mike shot ground-motion studies of Operation Ivy (Reference 5) were plotted on the same graph for comparison. It is evident that the same power law,

$$A = K\Delta p^{1.2}, \tag{3.1}$$

where A is peak acceleration, Δp is peak incident overpressure, and K is a coefficient, may be used to express the acceleration-overpressure relationship for both sets of data with the exception of different coefficients. The difference in coefficients, 0.144g for LaCrosse and 0.042g for Mike, is consistent with the fact that Mike data represent observations at a depth of 17.5 feet, but the LaCrosse data represent instrument reaction at an average depth of about 2.5 feet or less. The ratio of coefficients—about 3—is not unreasonable, but it must be recognized that it includes shot conditions which differ considerably and that yields which varied by a factor of one thousand resulted in much longer rise times for Mike pressures.

The rather sparse data for accelerations observed at 5- and 50-foot depths during Operation Tumbler-Snapper (Reference 3) show ratios of peak acceleration at the two depths ranging from about 2 to 10. But overpressure range, 0.5 to 10 psi, and differences in soil at Frenchman Flat and Eniwetok do not encourage quantitative comparison of these sets of data. It is interesting to note that the Tumbler-Snapper data follow, in general, the relationship,

$$A = 0.032\,\Delta p^{0.89},$$

in which the difference between the Δp exponent and that of Equation 3.1 may well, in part, express differences in response characteristics of the Nevada and Eniwetok soils.

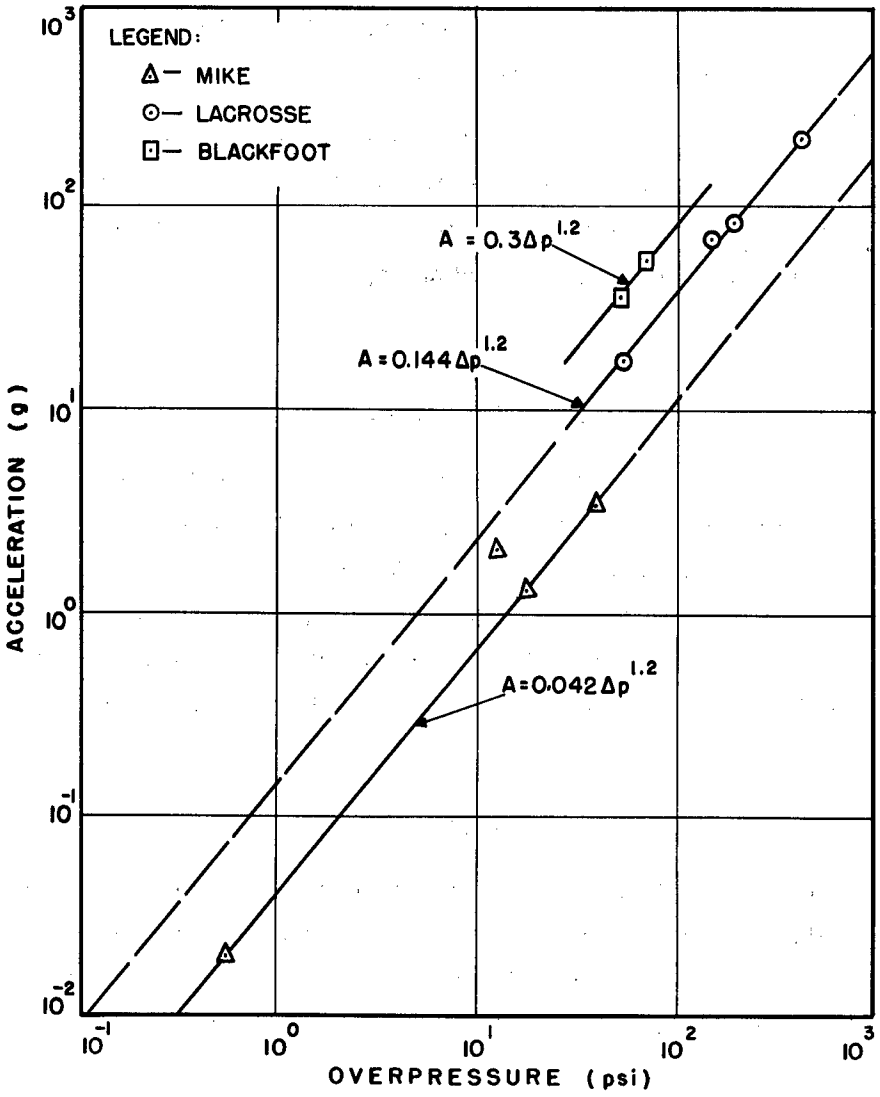

Figure 3.4 Peak ground acceleration versus peak incident overpressure.

The two peak accelerations observed for Blackfoot shot are hardly enough for independent analysis in terms of peak incident overpressures. However, a line on the graph (Figure 3.4), having the same slope as those representing LaCrosse and Mike data, passes reasonably close to the two Blackfoot points (squares), suggesting similar mechanisms in all three cases. The line may be described by

$$A = 0.3\ \Delta p^{1.2}. \qquad (3.2)$$

No good reason for the factor of 2 between the coefficient in Equation 3.2 and that for LaCrosse data is at first apparent. It is, of course, possible that the peak accelerations for the higher

pressure LaCrosse data were suppressed by perturbation earlier in the loading cycle than suggested above. L-3AV data show no evidence of such perturbation, even though they correlate with the peak accelerations at the perturbed stations. However, if it is assumed that the acceleration should scale as $W^{1/3}$, scaled Blackfoot data are wholly consistent with scaled LaCrosse data, using 1.6 times the radiochemical yield for the surface burst. The scaling assumption is tenable for air-induced ground motion, although rigorous analysis for the correct scaling relationship is not complete.

3.4 VELOCITY- AND DISPLACEMENT-TIME ANALYSIS

All acceleration-time records from canisters installed for LaCrosse and Blackfoot shots, with the exception of L-1AV, were integrated with respect to time. The resulting velocity-time data were integrated again, yielding displacement-time curves. Operation on data from LaCrosse shot accelerometer records was limited to that portion of the record following arrival of direct air-shock-induced motion. Earlier portions of the records were ignored in integration because uncertainties would have required manipulation, unjustifiable in view of the spurious features of the records after air-shock arrival. Records from Blackfoot canisters were remarkably clean and included evidence of arrival of ground-transmitted signals before those induced directly by air shock. Integration of each record in its entirety indicated complete ground motion for the recorded period. In all integrated records, some corrections for zero changes were necessary to produce internal consistency, but in no case did these corrections exceed a few percent of accelerometer set range; most corrections were less than 1 percent. Figure 3.5 represents only the acceleration data for L-1AV showing the limited range of useful record. Plots of the acceleration, velocity, and displacement data versus time are included in Figures 3.6 through 3.12. Maximum velocities and displacements are tabulated in Table 3.1, which includes data from the inertial scratch gages.

Data from the inertial scratch gages were not consistent or correlatable with integrated accelerations. Bending of the guide rods at Stations L-1/2 and L-2 made measured scratches of very doubtful value. At L-1/2, there is evidence of a scratch between 0.3 and 0.4 inch long, but the bent rod may have prevented further motion of the block. The 3.75-inch scratch record in Canister L-2, although possibly real, is more than an order of magnitude beyond the displacement derived from the acceleration data, which are not considered representative of canister motion beyond a few milliseconds after shock arrival. No correlation could be expected here. The scratch record for L-3 shows response to only about one fourth the downward motion indicated by integrated acceleration data from L-3AV. Scratch data only were derived from Canister L-4, but this information—twice the indicated displacement at L-3—does not correlate with other scratch-gage data.

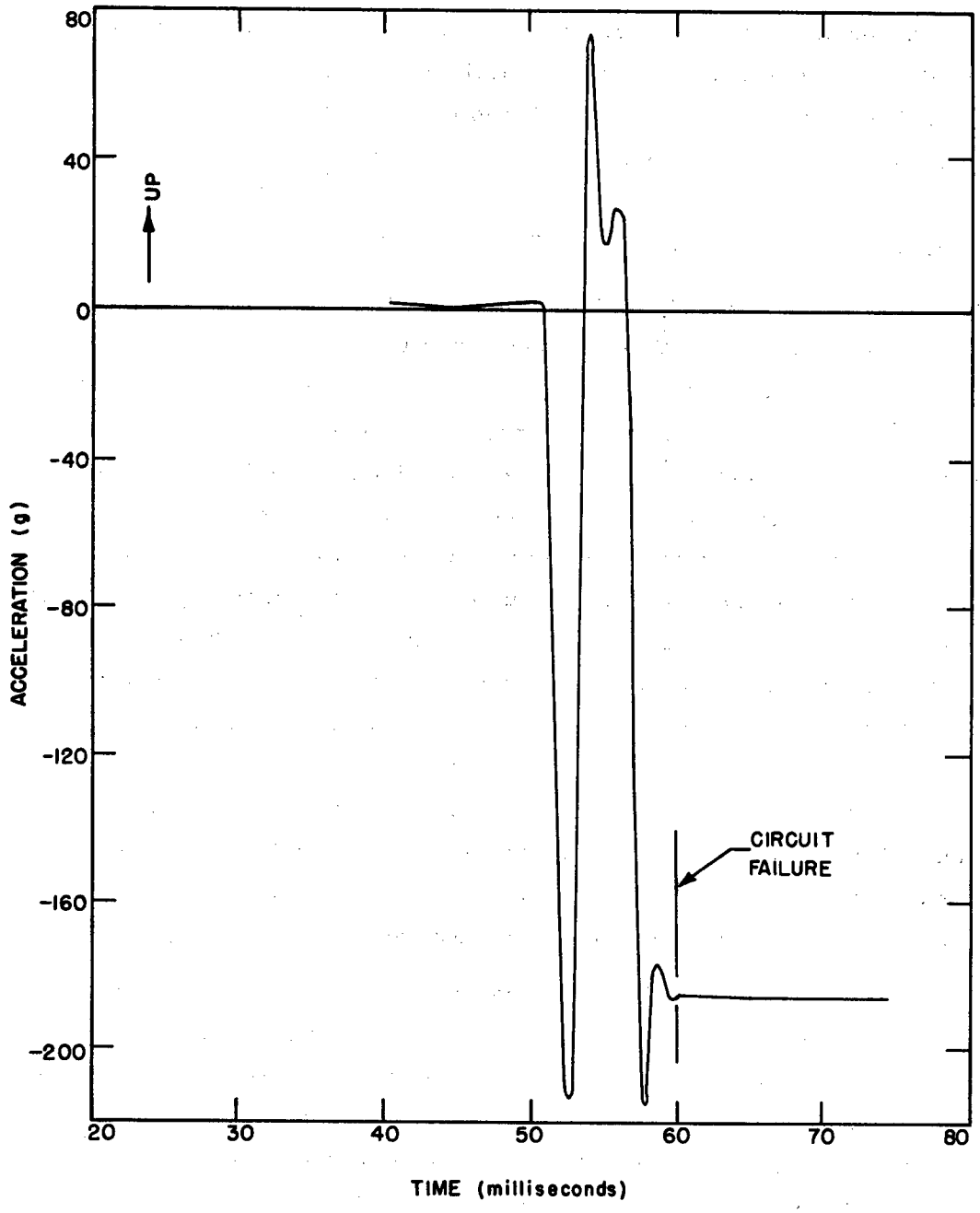

Figure 3.5 Vertical acceleration, Gage L-1AV, LaCrosse shot.

TABLE 3.1 MAXIMUM CANISTER VELOCITIES AND DISPLACEMENTS

Canister	Gage	Computed Velocity (ft/sec)	Computed Displacement (in.)	Direction	Inertial Gage Displacement (in.)
L-1/2	L-1/2AV	6.75	0.32	Down	0.4 (approx)
		6.08	3.83	Up	--
L-2	L-2AV	2.80	0.16	Down	3.75
		9.34	6.04	Up	--
	L-2AR	1.22	0.32	Out	--
		0.104	--	In	--
	L-2AT	0.63	0.031	Counterclockwise	--
		0.23	0.029	Clockwise	--
L-3	L-3AV	2.44	1.1	Down	0.3
		3.12		Down	--
		1.04	--	Up	
L-4	L-4AV	No Record	No Record	Down	0.6
B-1	B-1AV	3,54	0.360	Down	--
		0.46	0.095	Up	--
B-2	B-2AV	2.48	0.081	Down	--
		0.38	0.047	Up	--

Curves for Accelerometer L-1/2AV (Figure 3.6) and for Accelerometers L-2AV, L-2AR, and L-2AT (Figures 3.7, 3.8, and 3.9) show perturbations from thrust of guide rods against the underside of the central plate. Data from L-1/2AV include major disturbance in the period between about 3 and 12 milliseconds after shock arrival, with less significant effects continuing during an additional 10 milliseconds. These perturbations decreased the magnitude of the initial downward velocity pulse and enhanced the upward velocity, with consequent constraint of downward displacement derived by integration to about 0.4 inch and total apparent upward displacement of the order of 3.8 inches. The velocity curve suggests that if the perturbation had not occurred, displacements might have remained within 1 inch. A similar major disturbance, lasting about 8 milliseconds, appears in the three records from Station 3022. This is followed by weaker spurious signals throughout about 30 milliseconds. The appearance of velocity and displacement curves for Gage L-2AV (Figure 3.7) suggests that the major upward displacement is strongly influenced, as in L-1/2AV (Figure 3.6), by the guide-rod perturbation. Curves for Gages L-2AR and L-2AT (Figures 3.8 and 3.9) suggest similar, though perhaps not so significant, non-ground-motion influences.

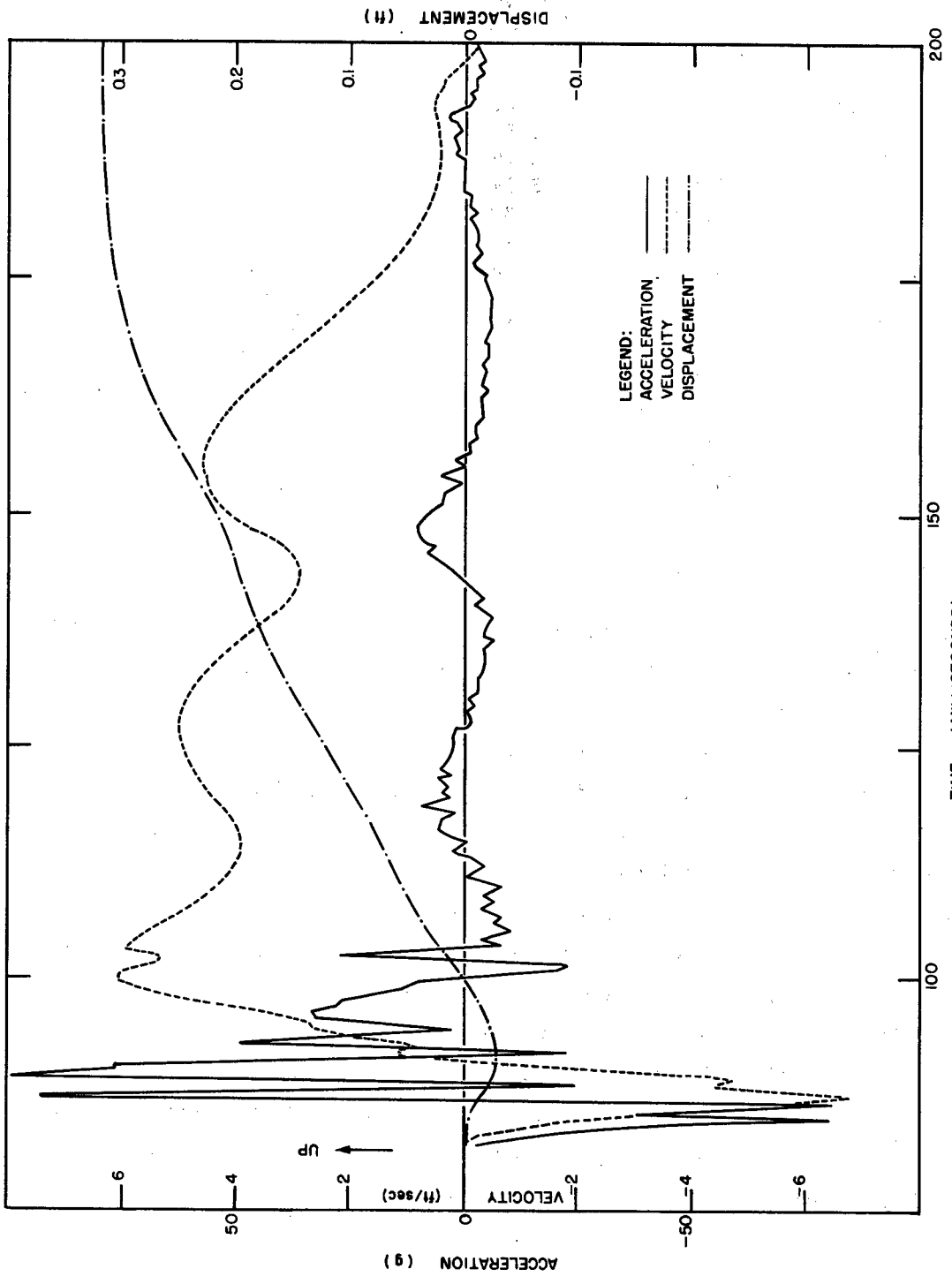

Figure 3.6 Vertical acceleration, velocity, displacement, Gage L-1/2AV, LaCrosse shot.

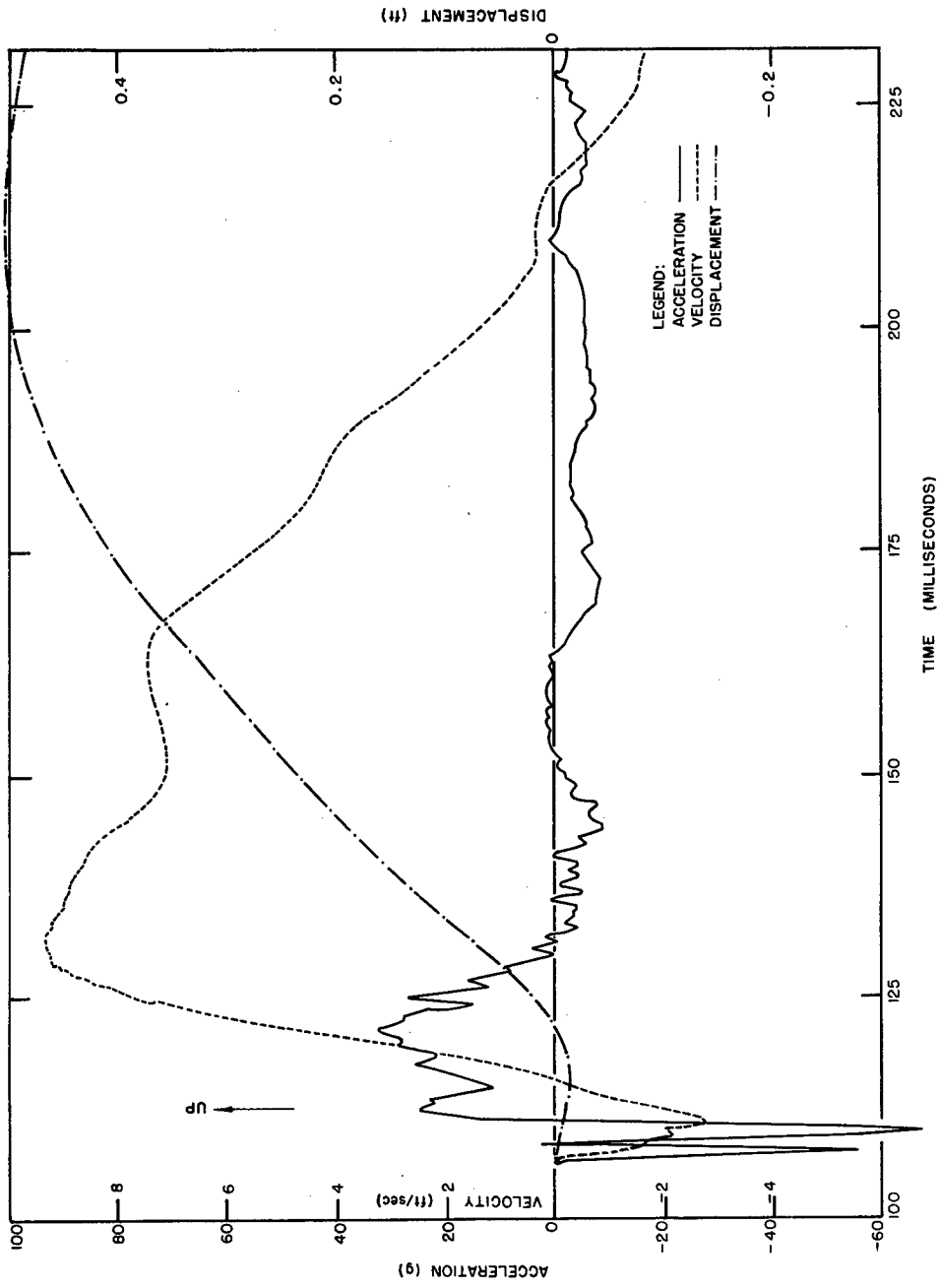

Figure 3.7 Vertical acceleration, velocity, displacement, Gage L-2AV, LaCrosse shot.

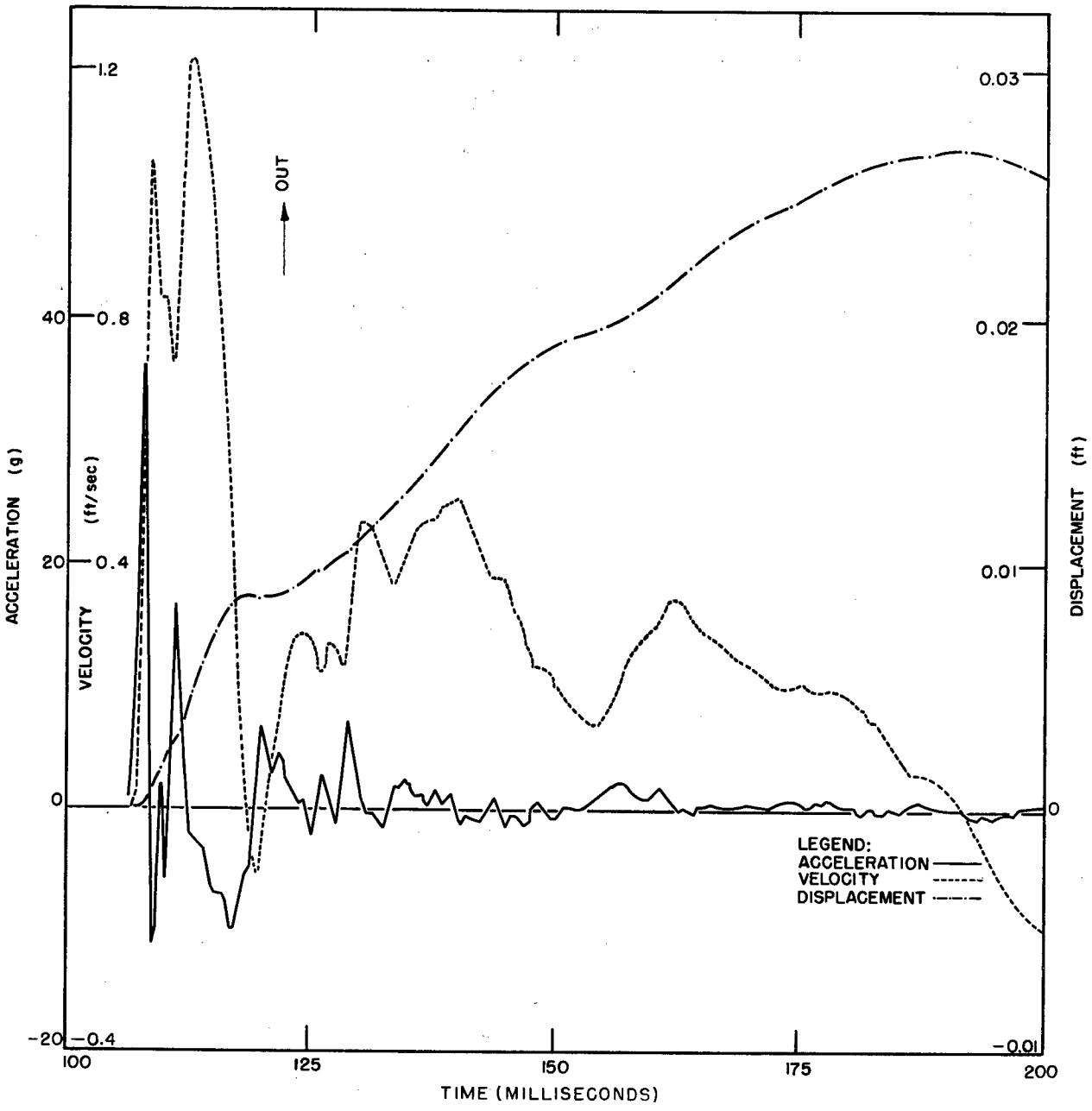

Figure 3.8 Radial acceleration, velocity, displacement, Gage L-2AR, LaCrosse shot.

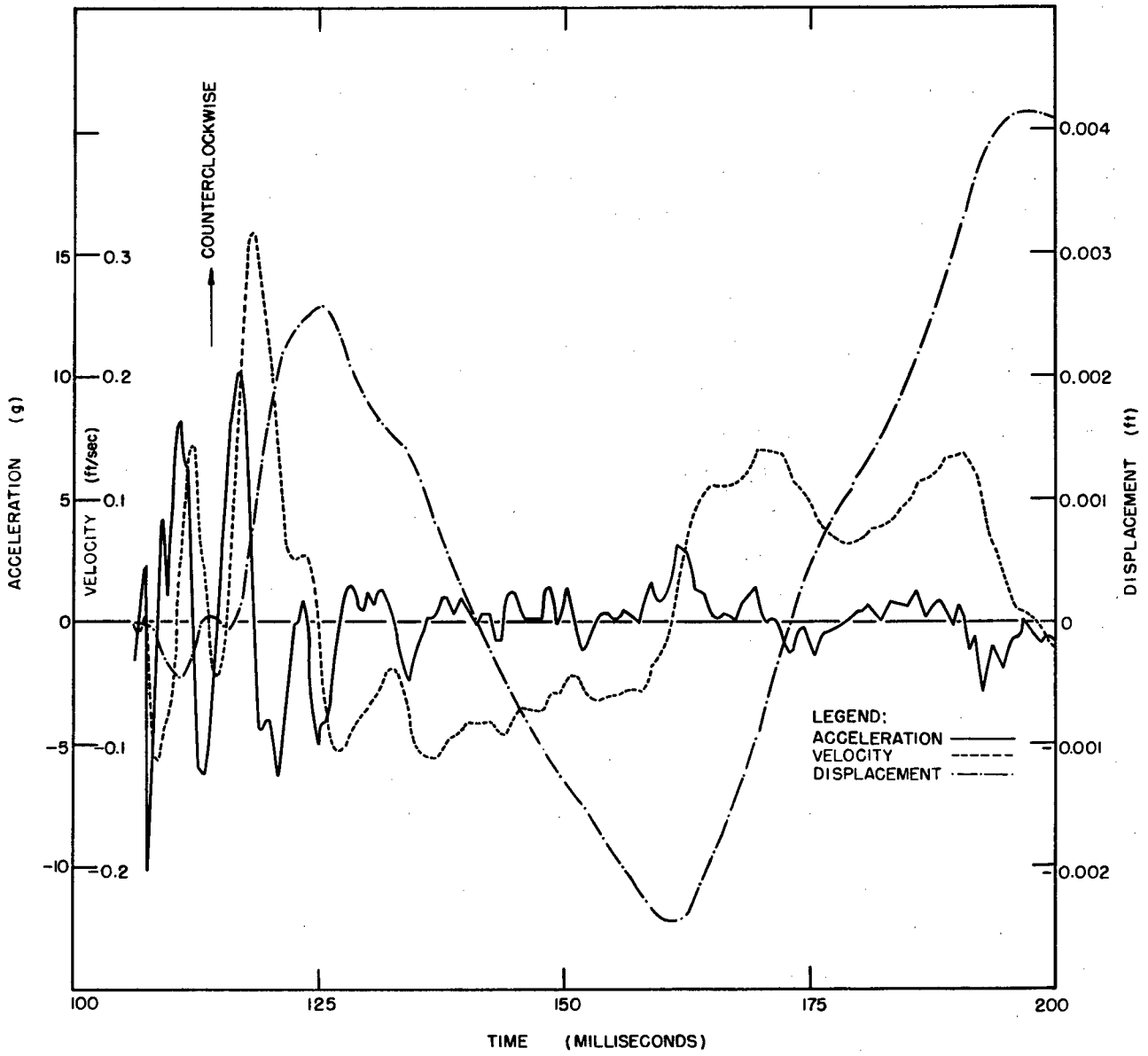

Figure 3.9 Tangential acceleration, velocity, displacement, Gage L-2AT, LaCrosse shot.

No extraneous effects such as occurred in the higher pressure level canisters appear on the records for Gage L-3AV or on the two Blackfoot records, B-1AV and B-2AV. Air overpressure data from the ground baffle gage at Station 3023 adjacent to the canister containing Accelerometer L-3AV include a precursor of about a 40-millisecond duration. Accelerometer L-3AV (Figure 3.10) gave a typical record for ground motion induced by air shock including a precursor: two downward acceleration peaks of about 17g and 16g corresponding to initial loading by precursor and mainshock. The resulting displacement curve shows only downward motion, but includes a step caused by the precursor at about 0.6 inch and a maximum displacement of about 1.1 inches. There does not appear to be much, if any, recovery of displacement during the time for which the data were integrated. Some later slow recovery may have occurred. However, it is probable that the dry sandy soil may have exerted no significant restoring force so that downward displacement is essentially permanent.

The results of integrating the entire records from Canisters B-1 and B-2 (Figures 3.11 and 3.12) show low-frequency, low-amplitude displacement caused by ground-transmitted energy, upon which is imposed a downward displacement produced by air shock. Both records are similar, but the air-shock signal in the B-1AV record includes a broader initial downward component and a broader, more distinct upward portion than does the record from B-2AV. This is consistent with the incident overpressure records (Figure 3.13) in which the B-GB1 overpressure pattern includes a more rounded peak than that for B-GB2. This difference in air-shock acceleration durations causes downward velocity pulses of 16.5 milliseconds for B-1AV and only 8 milliseconds for B-2AV, with corresponding displacements of 0.060 foot and 0.0076 foot. The contributions of sharp higher peak pressures and greater induced peak accelerations to displacement are overshadowed by effects of pulse duration differences.

Data show a sufficiently distinct pattern in the velocity-time curve to permit separation of the ground-transmitted and air-shock-induced components. This has been done for B-1AV data in Figure 3.14, in which the velocity curve is reproduced and a dotted curve sketched in estimating velocities in the absence of air shock. In the same figure, the dash-dot displacement curve has been amended by a dashed portion representing the assumption of no air-shock-induced motion. Similar treatment of data from B-2AV is feasible, and the results (Figure 3.15) show distinctly the one-way downward displacement caused by air shock, as compared with the recovered or oscillatory upward displacement transmitted through the ground.

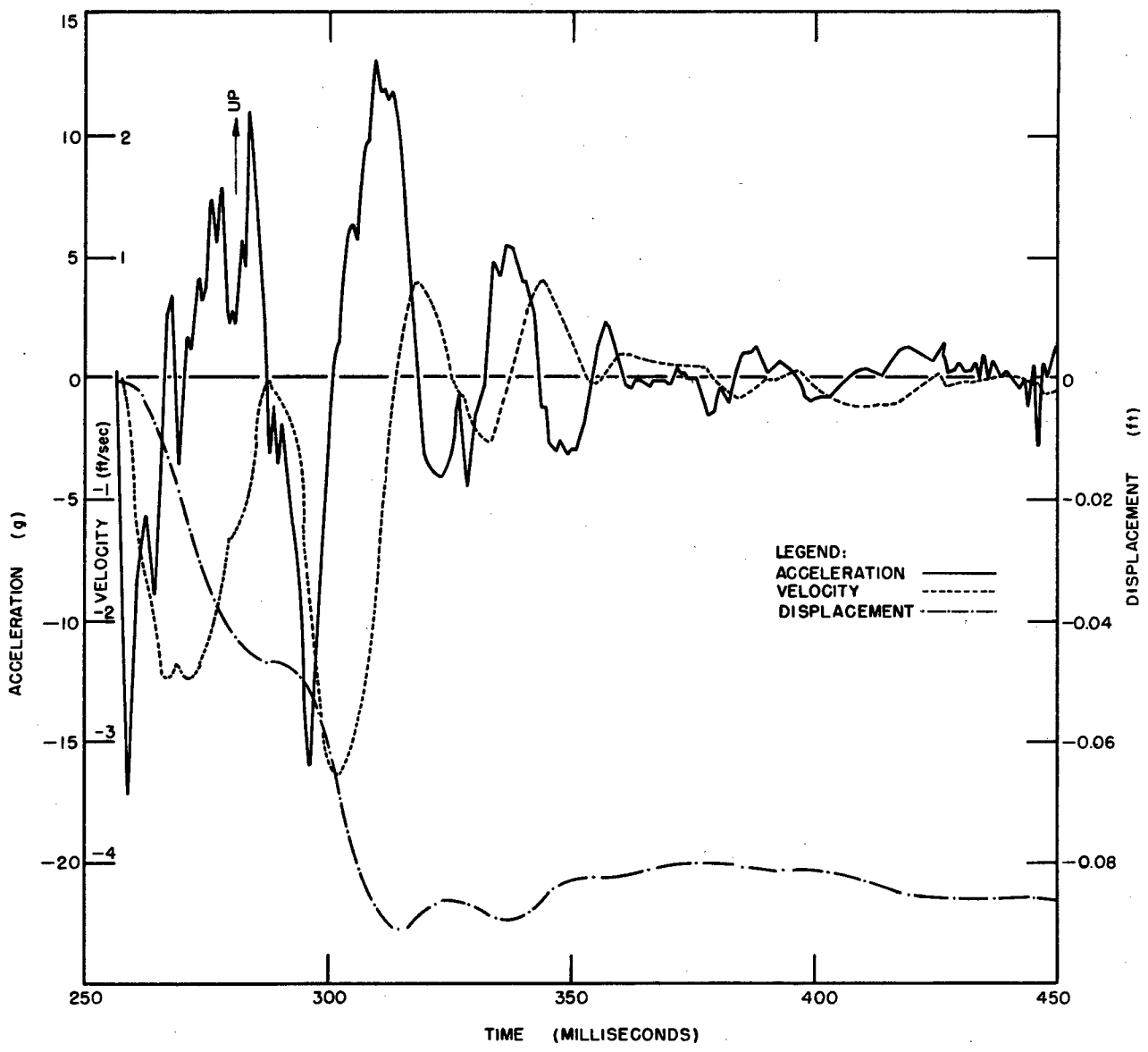

Figure 3.10 Vertical acceleration, velocity, displacement, Gage L-3AV, LaCrosse shot.

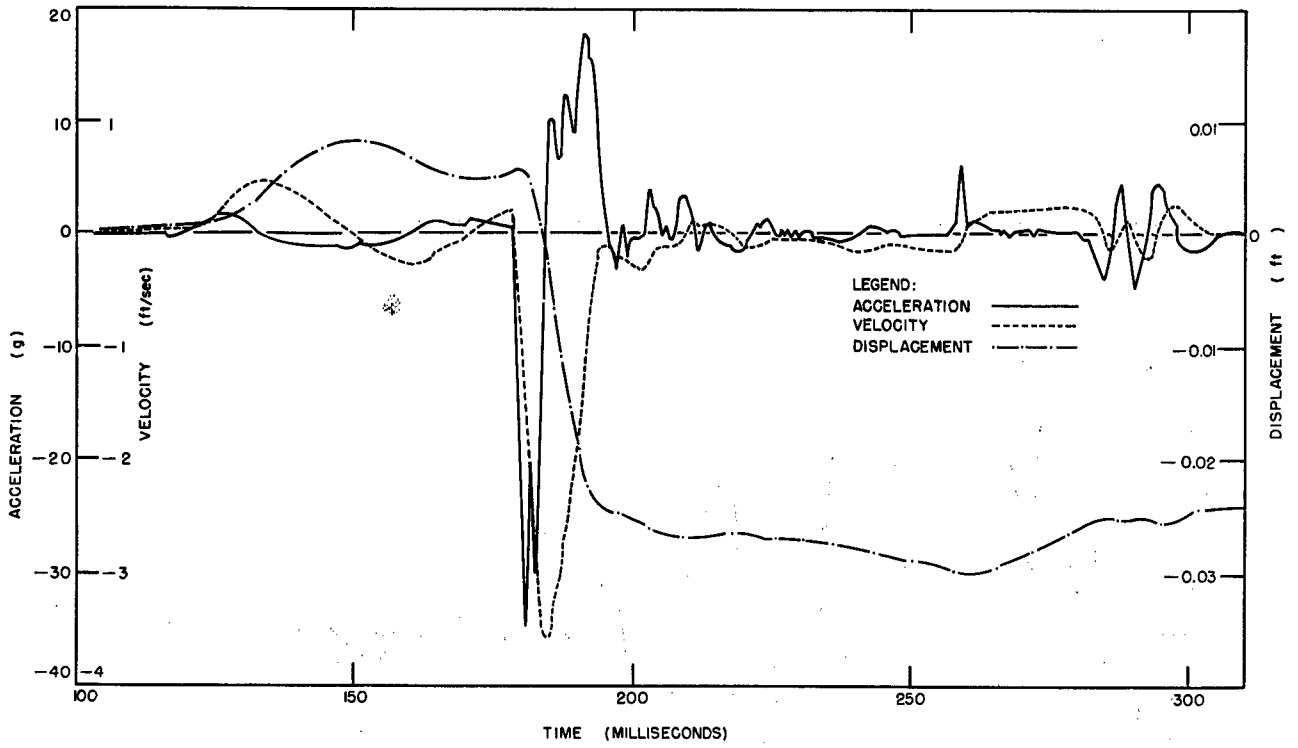

Figure 3.11 Vertical acceleration, velocity and displacement versus time, Gage B-1AV, Blackfoot shot.

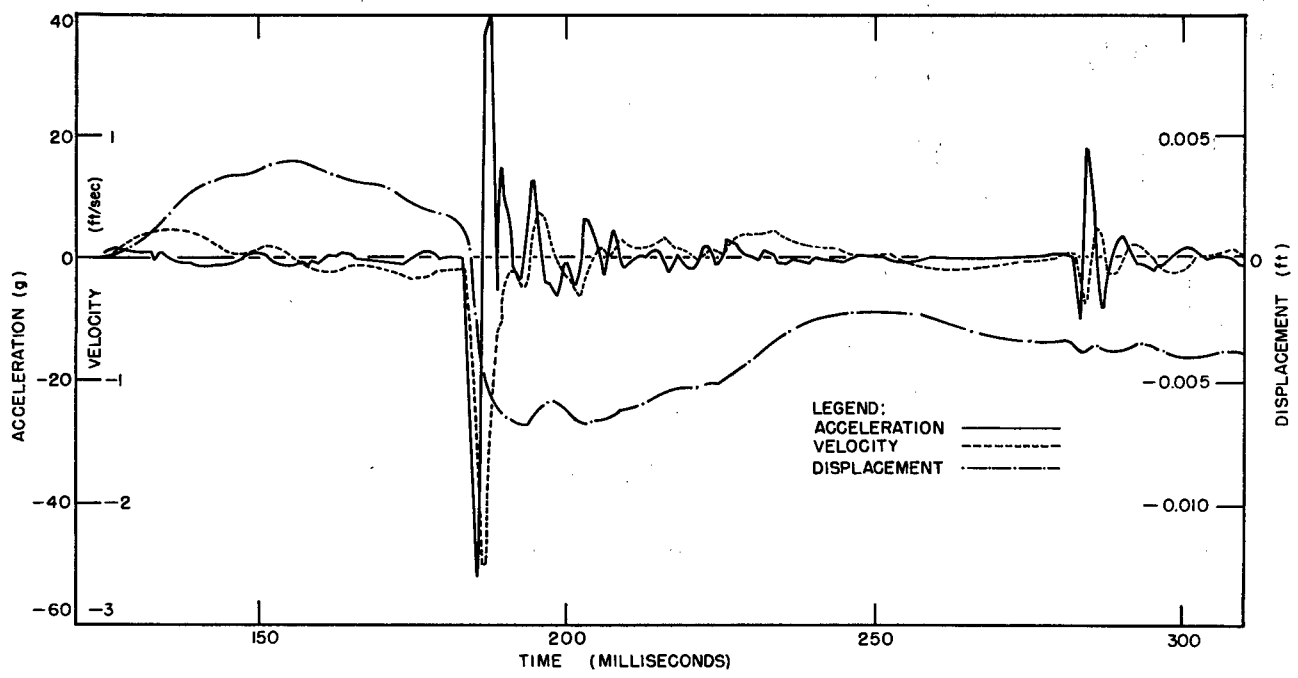

Figure 3.12 Vertical acceleration, velocity and displacement versus time, Gage B-2AV, Blackfoot shot.

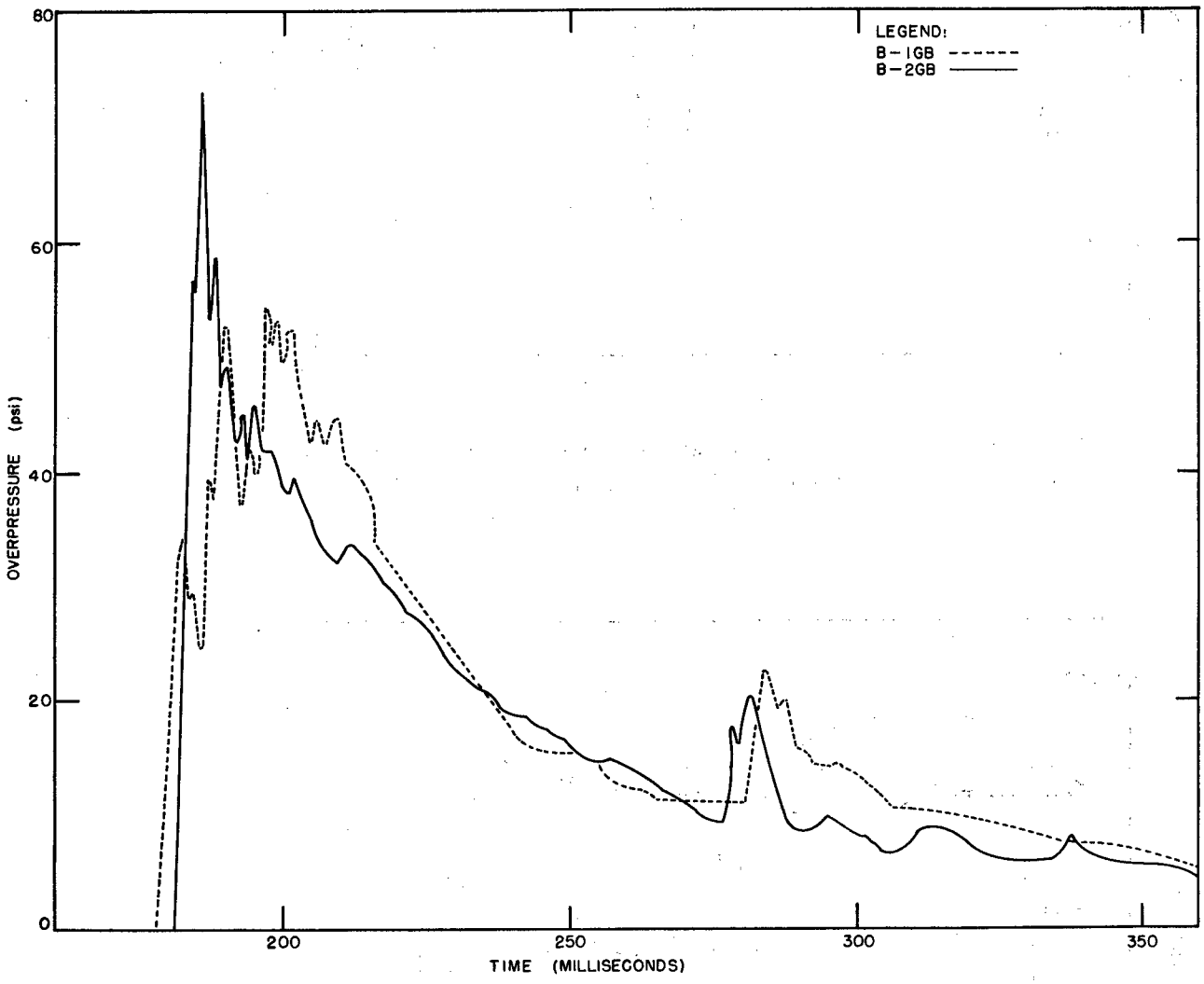

Figure 3.13 Ground baffle overpressure versus time, Blackfoot shot.

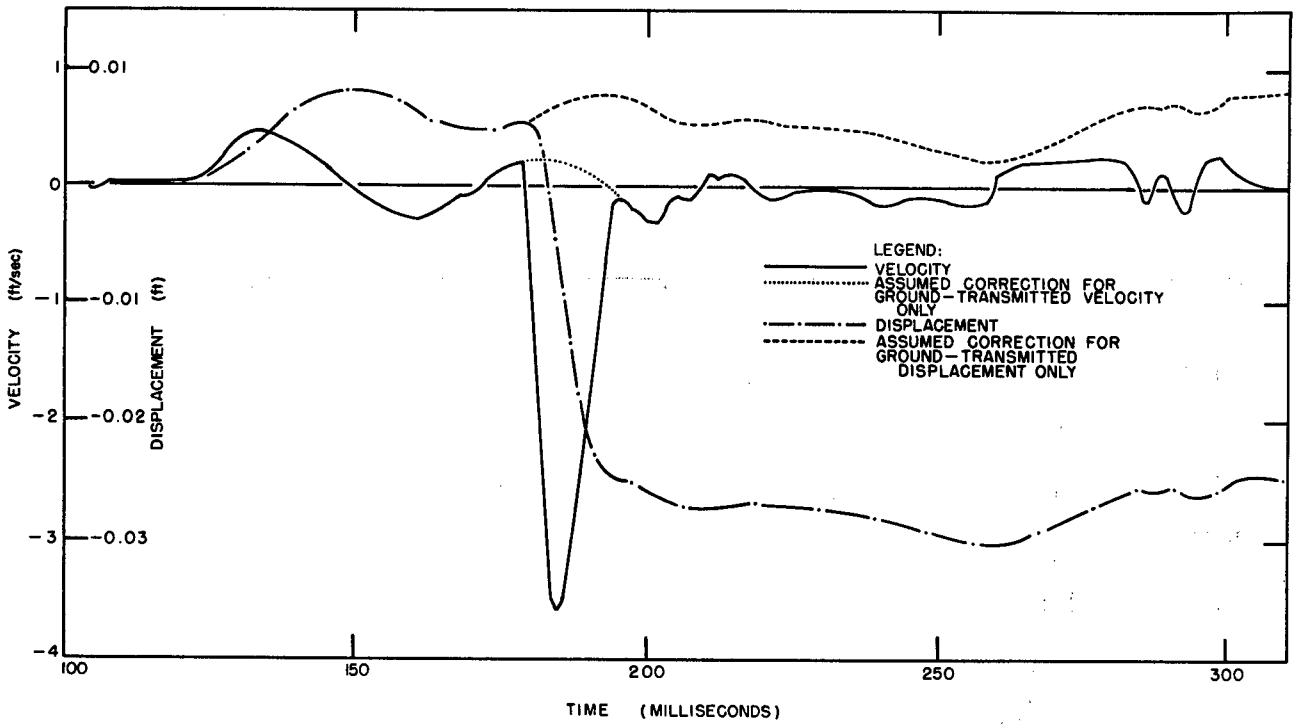

Figure 3.14 Resolution of air-shock and ground-transmitted components of vertical velocity and displacement, Gage B-1AV.

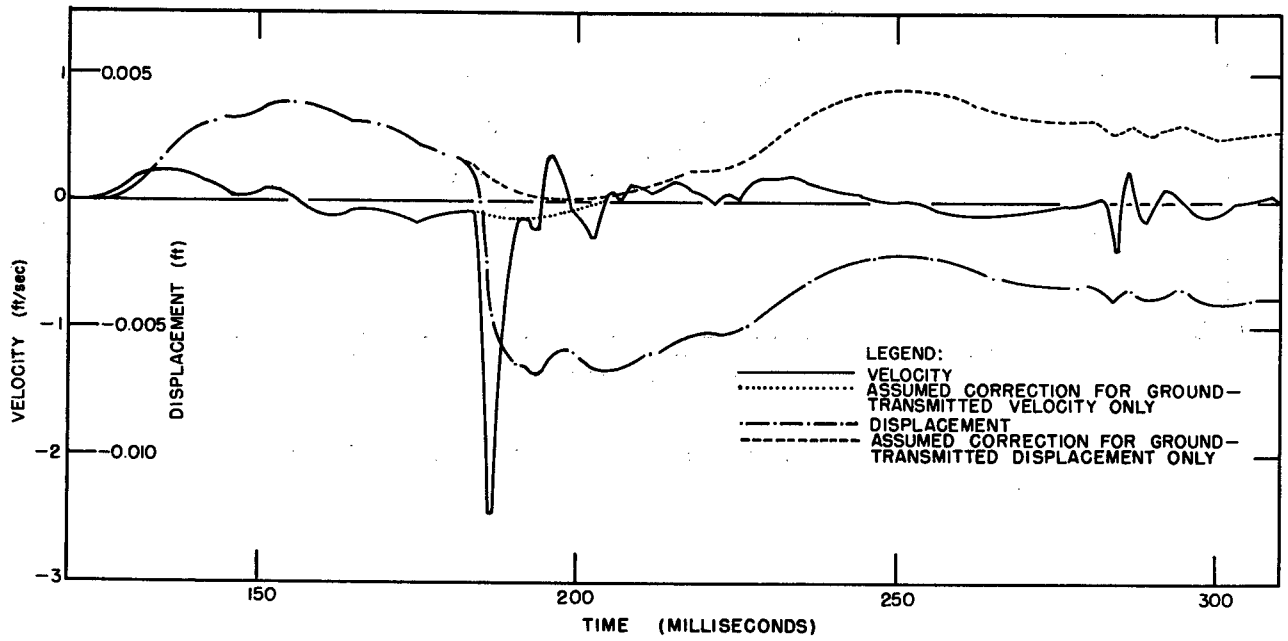

Figure 3.15 Resolution of air-shock and ground-transmitted components of vertical velocity and displacement, Gage B-2AV.

3.5 ACCELERATION SPECTRA

Acceleration-frequency spectra were derived for each canister acceleration record. Such a spectrum represents, for each of a series of frequencies, the maximum accelerations to which a simple mechanical oscillator of the specified natural frequency would be driven by an external force having the recorded acceleration-time parameter.

Spectra were derived from an analog computer (REAC). The analog element was a simple linear oscillator circuit which could be tuned through a range of discrete frequencies. The input signal comprised a voltage-time function representing the acceleration-time data for a specific canister component. Direct output of the analog element was a sine function of amplitude dependent on the input function. The relevant parameter for the spectrum is maximum acceleration, which the computer derives as $\omega^2 y$ from the sine function output, $y \sin \omega t$, of the oscillator circuit. The resulting spectrum is a plot of maximum $\omega^2 y$ versus frequency, ω, derived by running the input signal through the computer tuned to each discrete frequency.

Spectra were derived for each input function at three oscillator-damping conditions: zero damping and at 3 and 10 percent of critical damping.

Acceleration spectra for LaCrosse shot canisters are presented in Figures 3.16 through 3.20. Corresponding spectra for Blackfoot accelerometers are included in Figure 3.21. Spectra for the LaCrosse shot data in which guide rod perturbations are present include relatively stronger induced accelerations at high frequencies (above 400 cps) than do the unperturbed data for L-3AU and the two Blackfoot stations.

Velocity spectra may be derived from acceleration spectra by dividing the $\omega^2 y$ amplitudes (acceleration values) by frequency to obtain the ωy velocity terms as a function of frequency. Similarly, a displacement spectrum may be derived from an acceleration spectrum through division of $\omega^2 y$ by ω^2 to produce displacement amplitude, y, as a function of frequency.

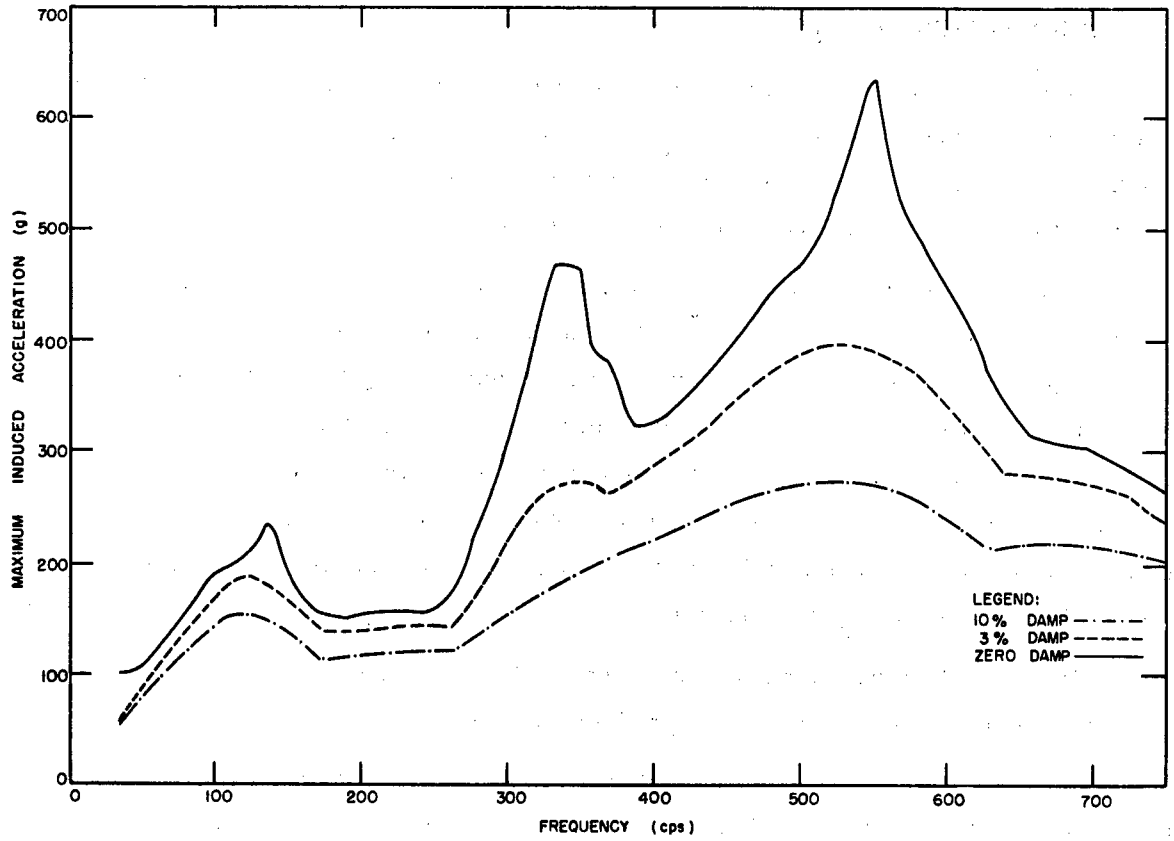

Figure 3.16 Acceleration spectra, Gage L-1/2AV, LaCrosse shot.

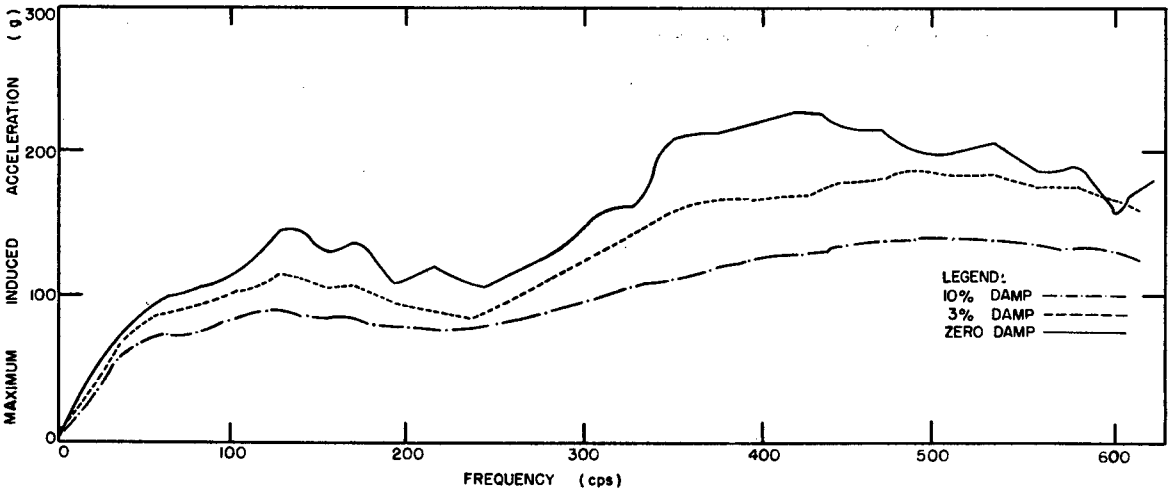

Figure 3.17 Acceleration spectra, Gage L-2AV, LaCrosse shot.

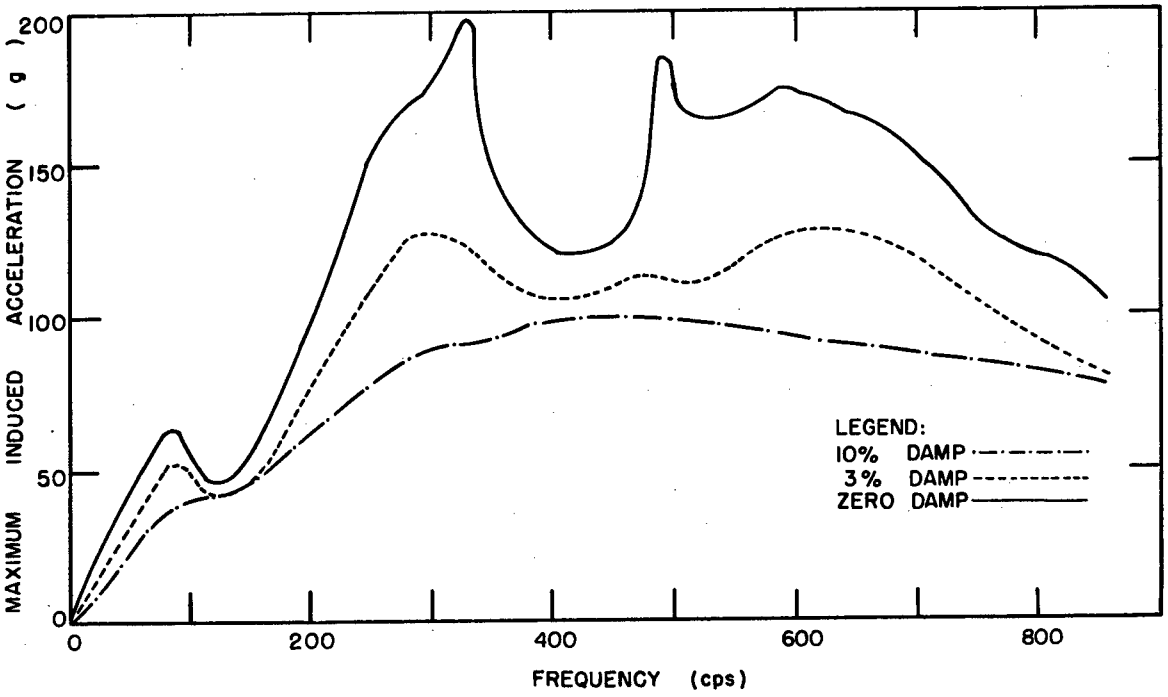

Figure 3.18 Acceleration spectra, Gage L-2AR, LaCrosse shot.

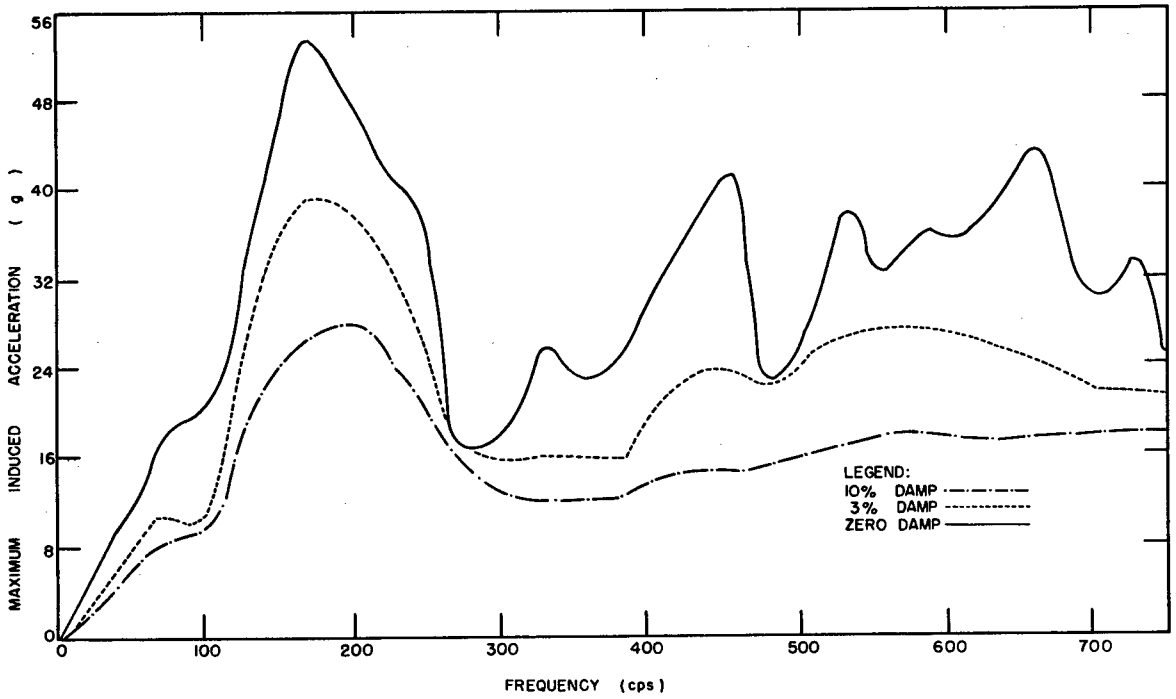

Figure 3.19 Acceleration spectra, Gage L-2AT, LaCrosse shot.

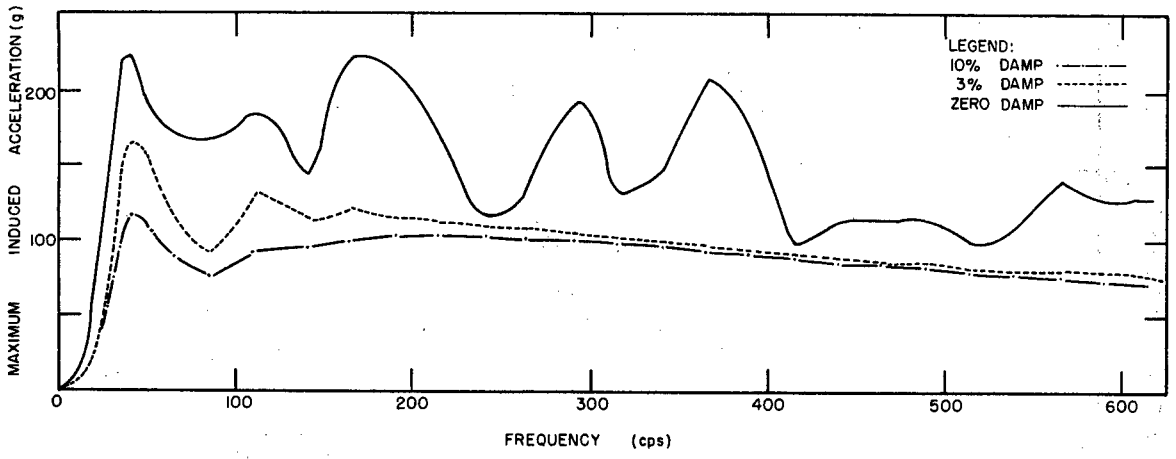

Figure 3.20 Acceleration spectra, Gage L-3AV, LaCrosse shot.

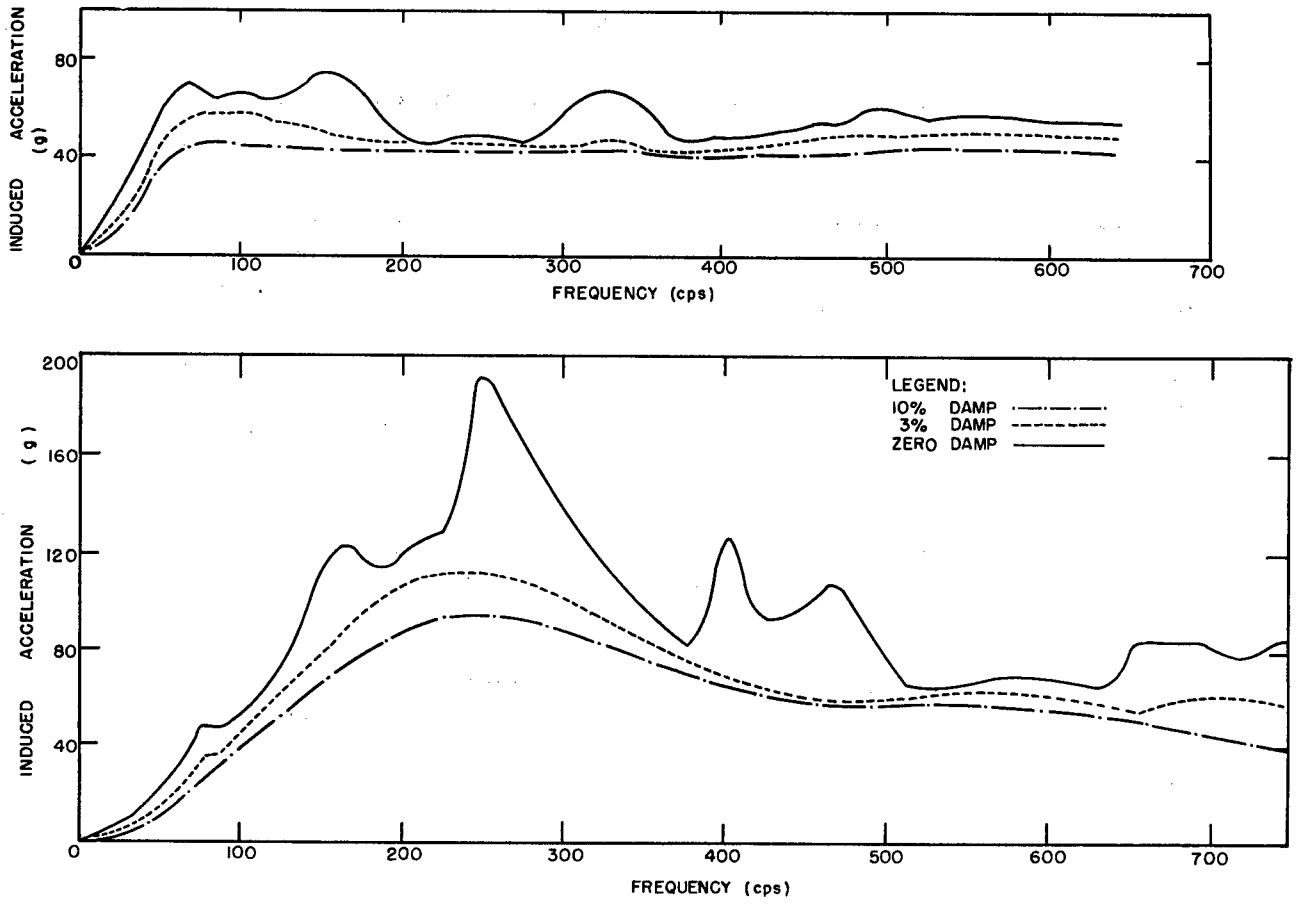

Figure 3.21 Acceleration spectra, Gages B-1AV (upper) and B-2AV (lower), Blackfoot shot.

[redacted]

CHAPTER 4

CONCLUSIONS

Ground-motion data from the buried mock-up telemeter canisters installed during LaCrosse and Blackfoot shots of Operation Redwing were not sufficiently free of perturbations to allow thorough analysis of ground motion. However, peak accelerations, which are probably free of perturbations, indicate that for Eniwetok coral sand, peak accelerations induced by air shock vary linearly with the 1.2 power of peak overpressure. This agrees with the corresponding data, at lower overpressures, derived from Mike shot of Operation Ivy. Differences in coefficients for the two empirical relations,

$$A = 0.144\ \Delta p^{1.2} \quad \text{for Operation Redwing (LaCrosse) and}$$

$$A = 0.042\ \Delta p^{1.2} \quad \text{for Operation Ivy (Mike),}$$

may be attributable to the greater depth of the instruments which yielded the Ivy-Mike data.

Data from three canisters, L-3 for LaCrosse and B-1 and B-2 for Blackfoot, were free of serious perturbation and represent real ground motion during the recorded period. Records from Gages B-1AV and B-2AV show distinctly the relatively greater displacement effect traceable to the more rounded overpressure curve observed at B-GB1 than that produced by the sharper curve derived at B-GB2.

Displacements indicated by inertial scratch gages were probably limited by bent guide rods in two canisters and were neither internally consistent nor correlatable with displacements derived from acceleration-time data in any of the four recovered canisters.

APPENDIX A

ACCELERATION SPECTRA: PROJECT 6.5, OPERATION IVY, AND PROJECT 1.4, OPERATION UPSHOT-KNOTHOLE

Three components of ground acceleration were observed at several ground ranges for Mike shot of Operation Ivy and at a single station for Shots 9 and 10 of Operation Upshot-Knothole. The data were analyzed and transformed to velocity- and displacement-time information where feasible. These results were published in WT-716, Operation Upshot-Knothole (Reference 4), and in WT-9002, Operation Ivy (Reference 5).

Design of underground protective structures has more recently introduced requirement for knowledge of free-field motion frequencies as defined by acceleration or velocity spectra to serve as input parameters, either for design of structures or for design of isolation of structure contents. To satisfy part of this requirement, acceleration spectra were derived from acceleration-time data for two Ivy-Mike stations and for the Upshot-Knothole station on Shots 9 and 10 as described in Section 3.4. Results of this analysis are presented in Figures A.1, A.2, A.3, A.4, A.5, and A.6 for Ivy-Mike data; Figures A.7, A.8, and A.9 for Upshot-Knothole Shot 1; Figures A.10, A.11, and A.12 for Upshot-Knothole Shot 9; and Figures A.13, A.14, and A.15 for Upshot-Knothole Shot 10.

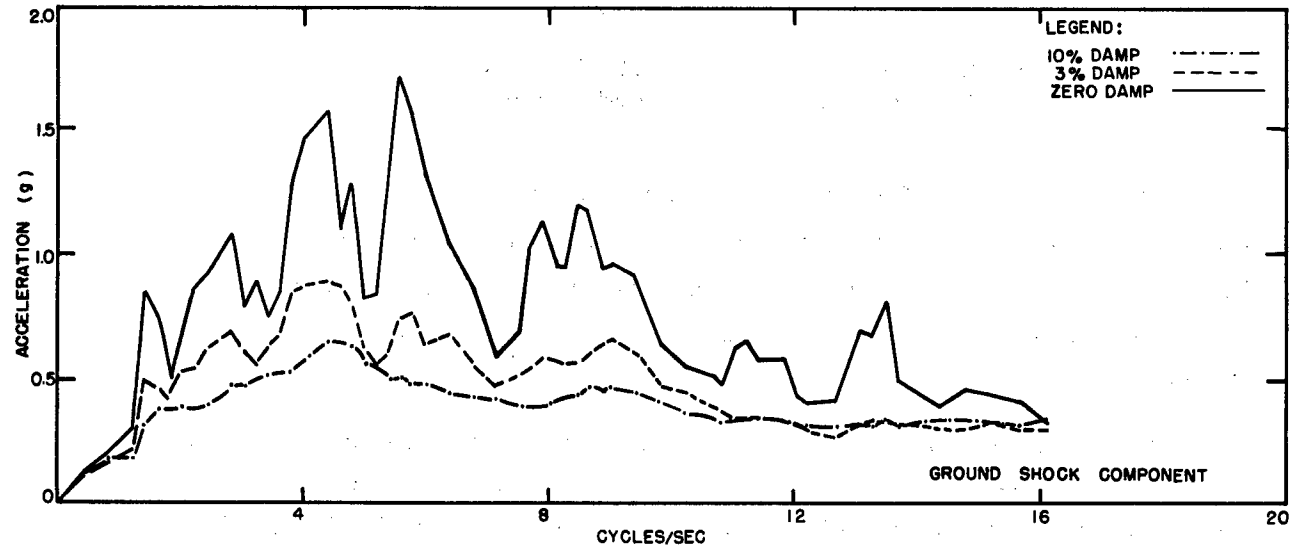

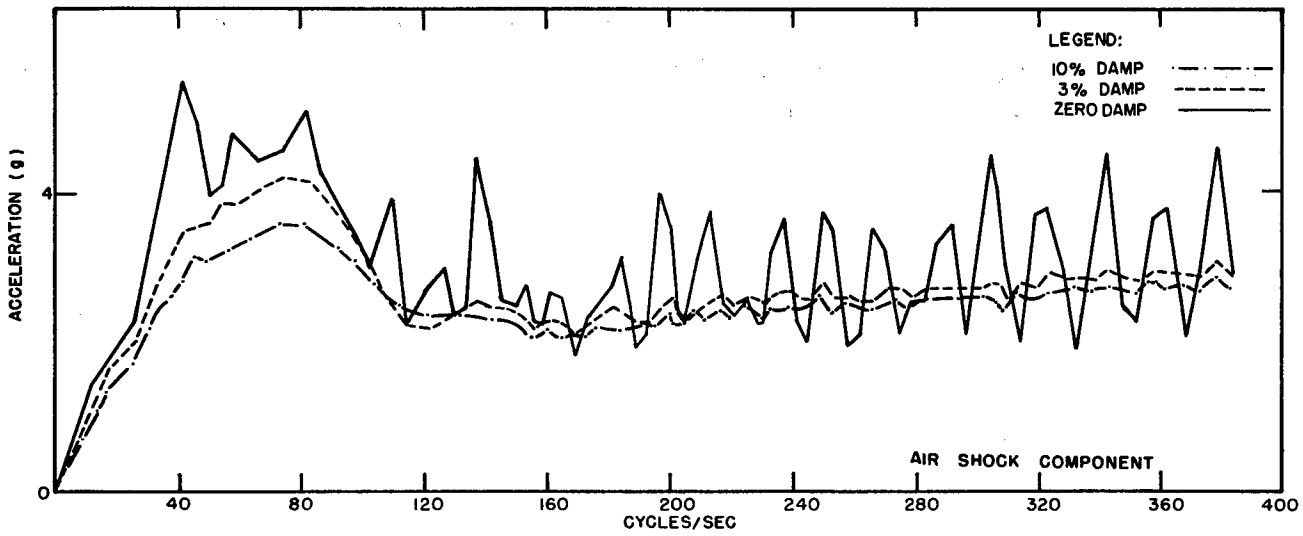

Figure A. 1 Vertical acceleration spectra, Station Janet, Operation Ivy.

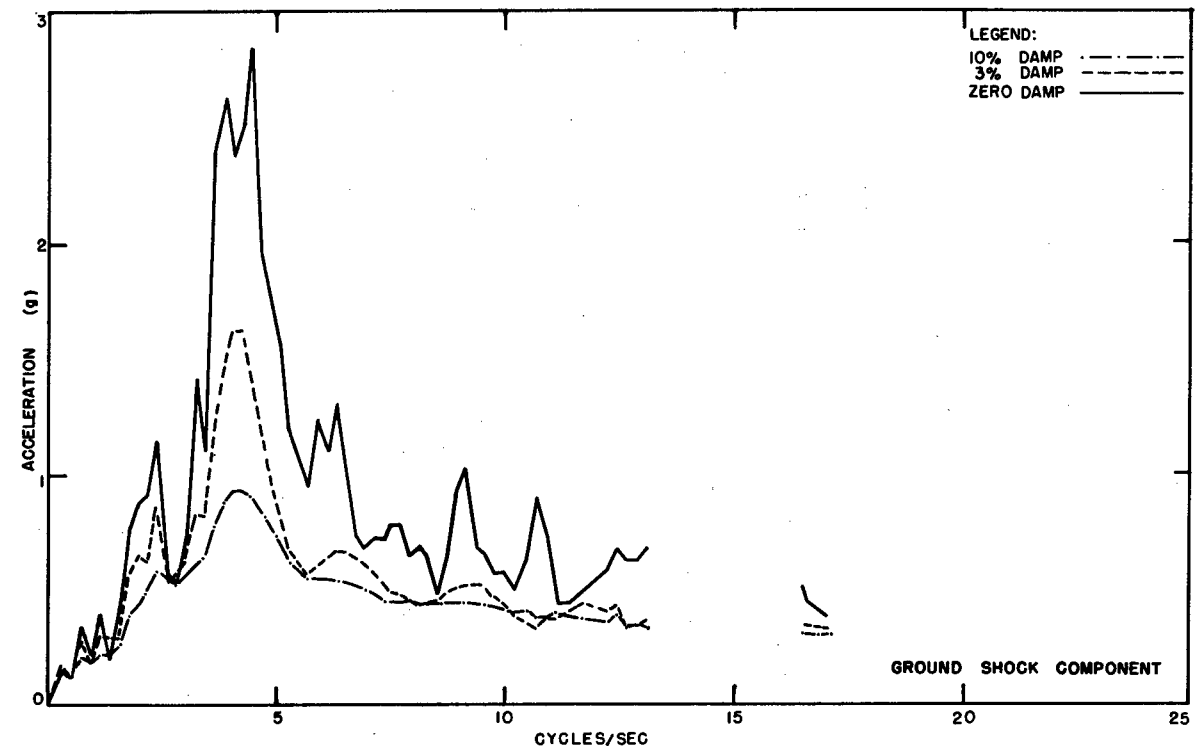

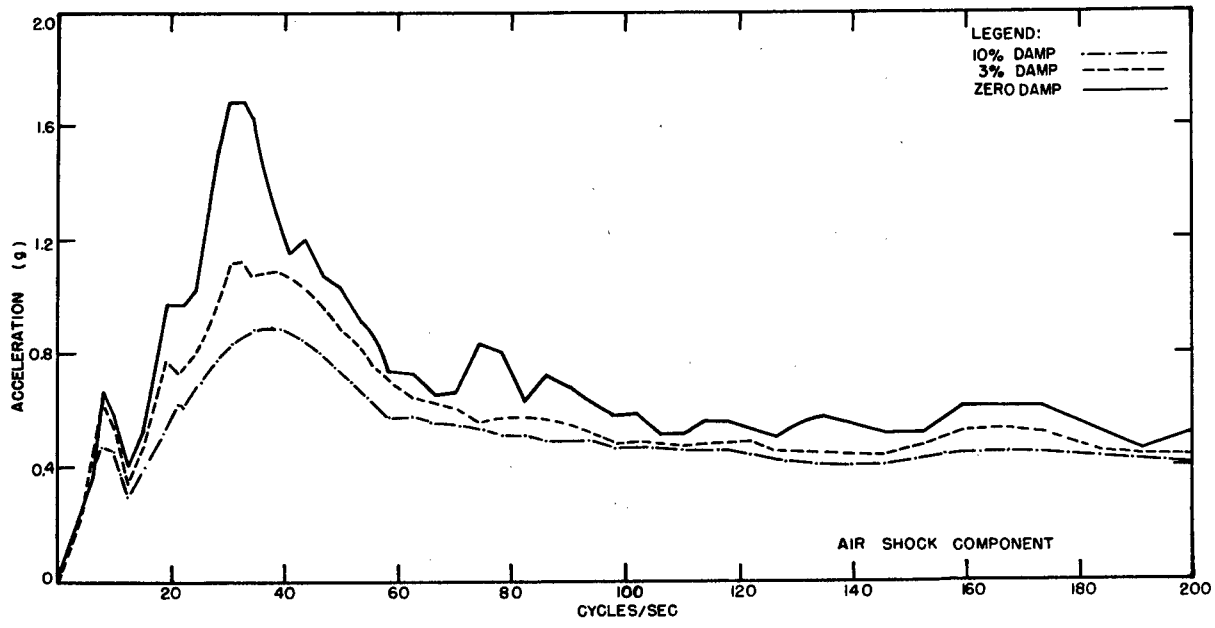

Figure A. 2 Radial acceleration spectra, Station Janet, Operation Ivy.

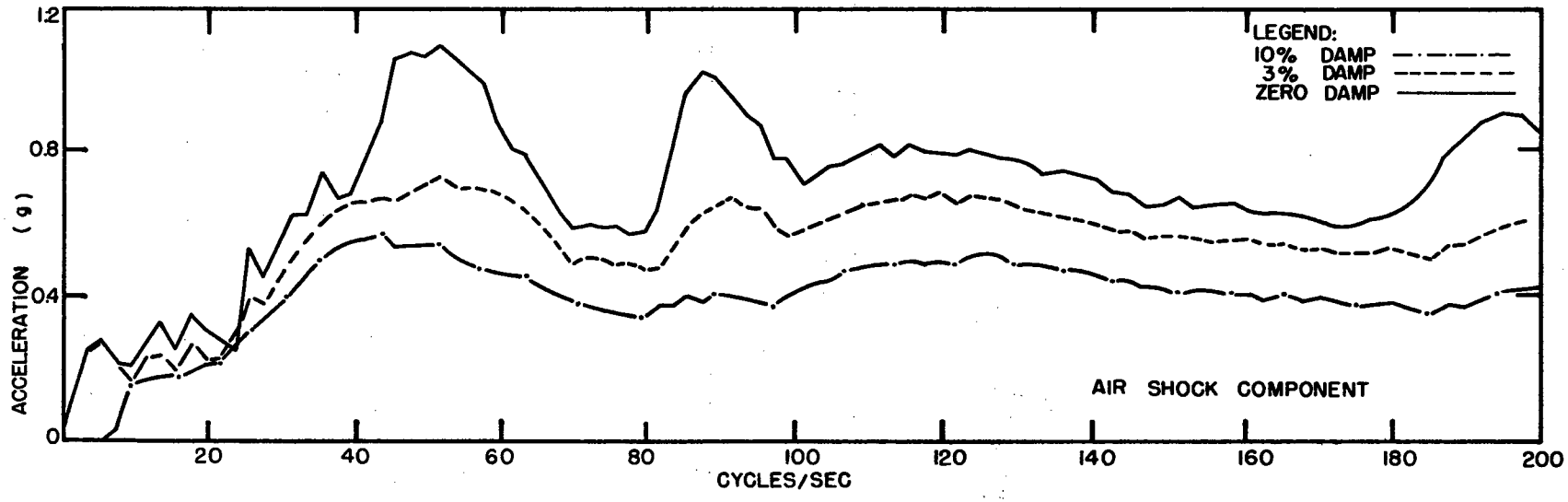

Figure A. 3 Tangential acceleration spectra, Station Janet, Operation Ivy.

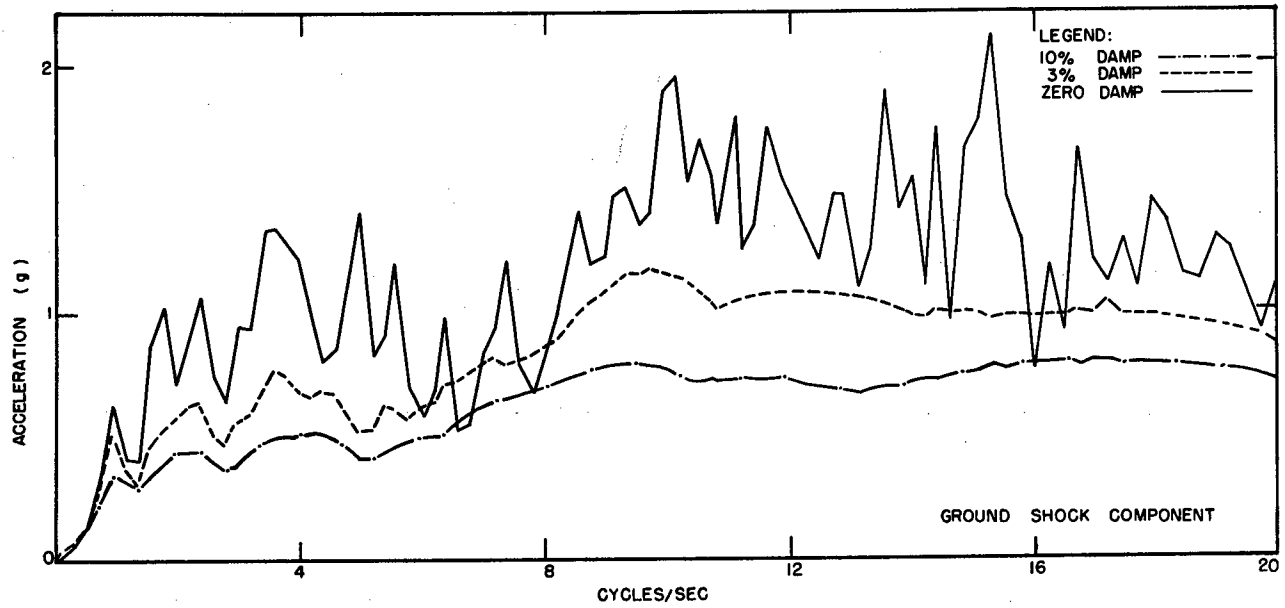

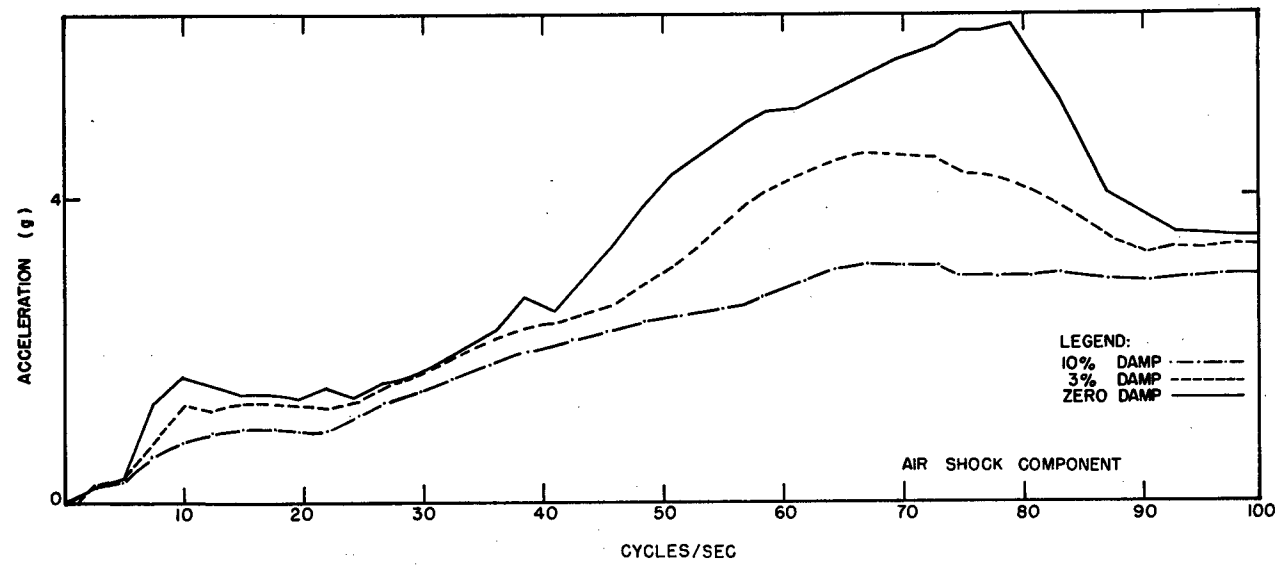

Figure A.4 Vertical acceleration spectra, Station Kate, Operation Ivy.

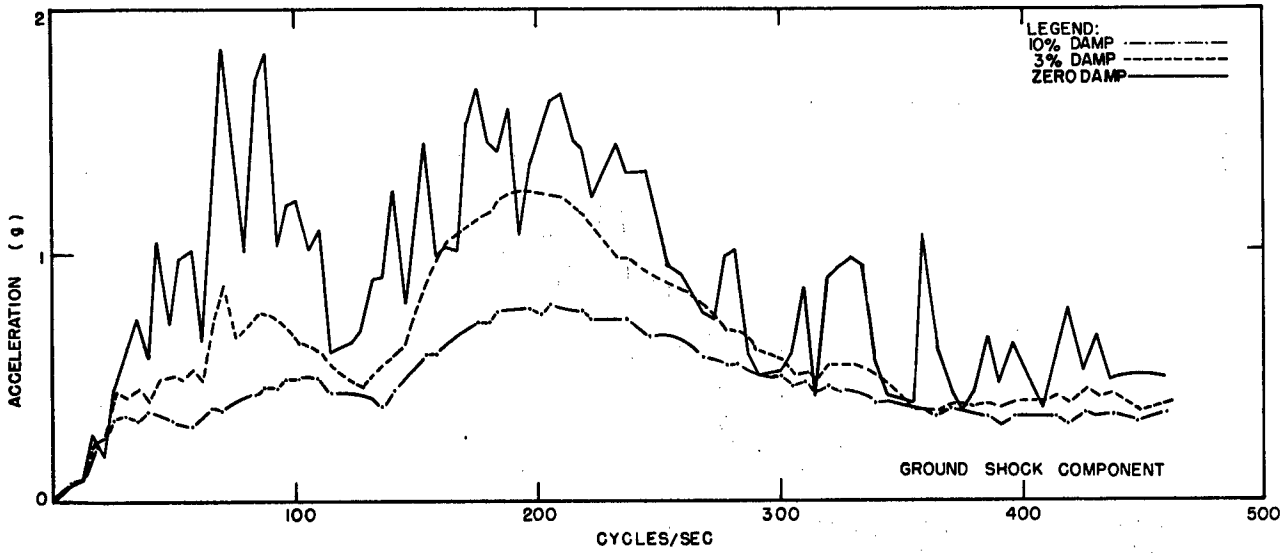

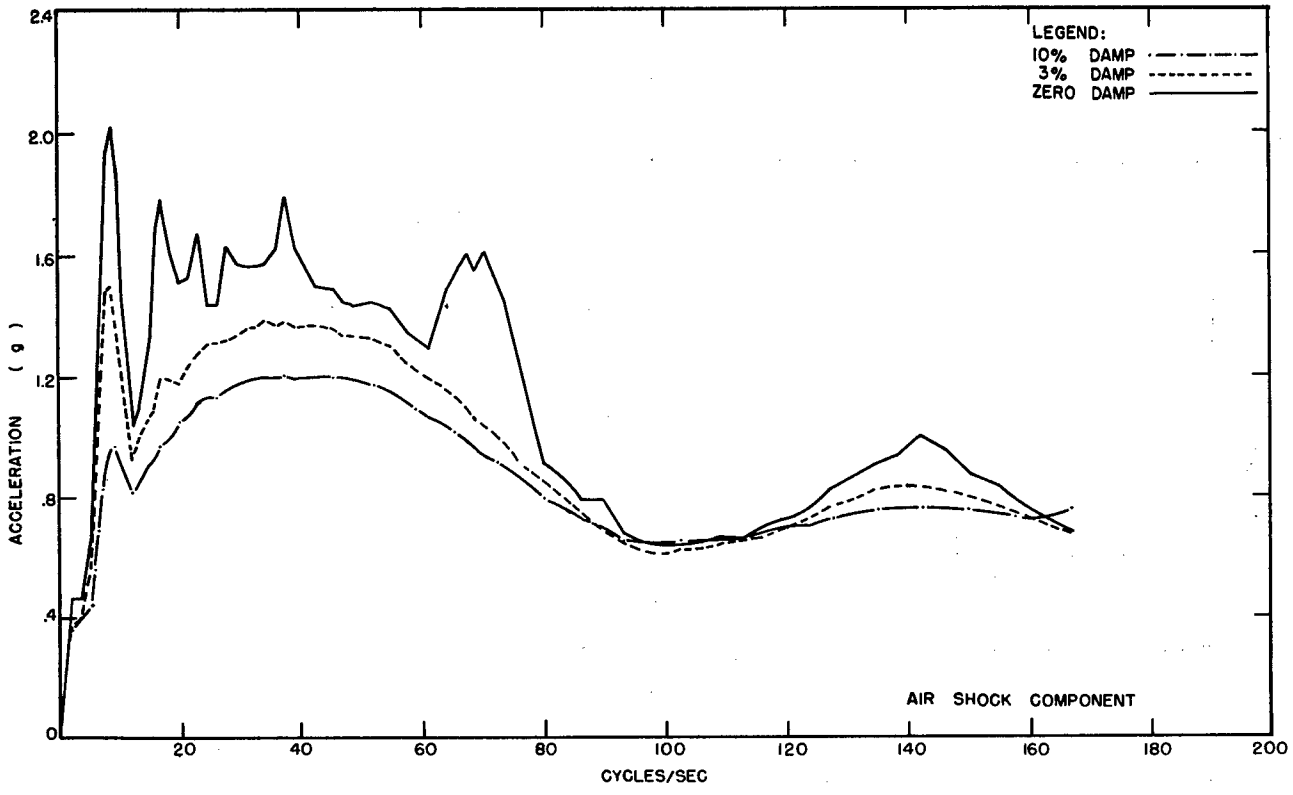

Figure A. 5 Radial acceleration spectra, Station Kate, Operation Ivy.

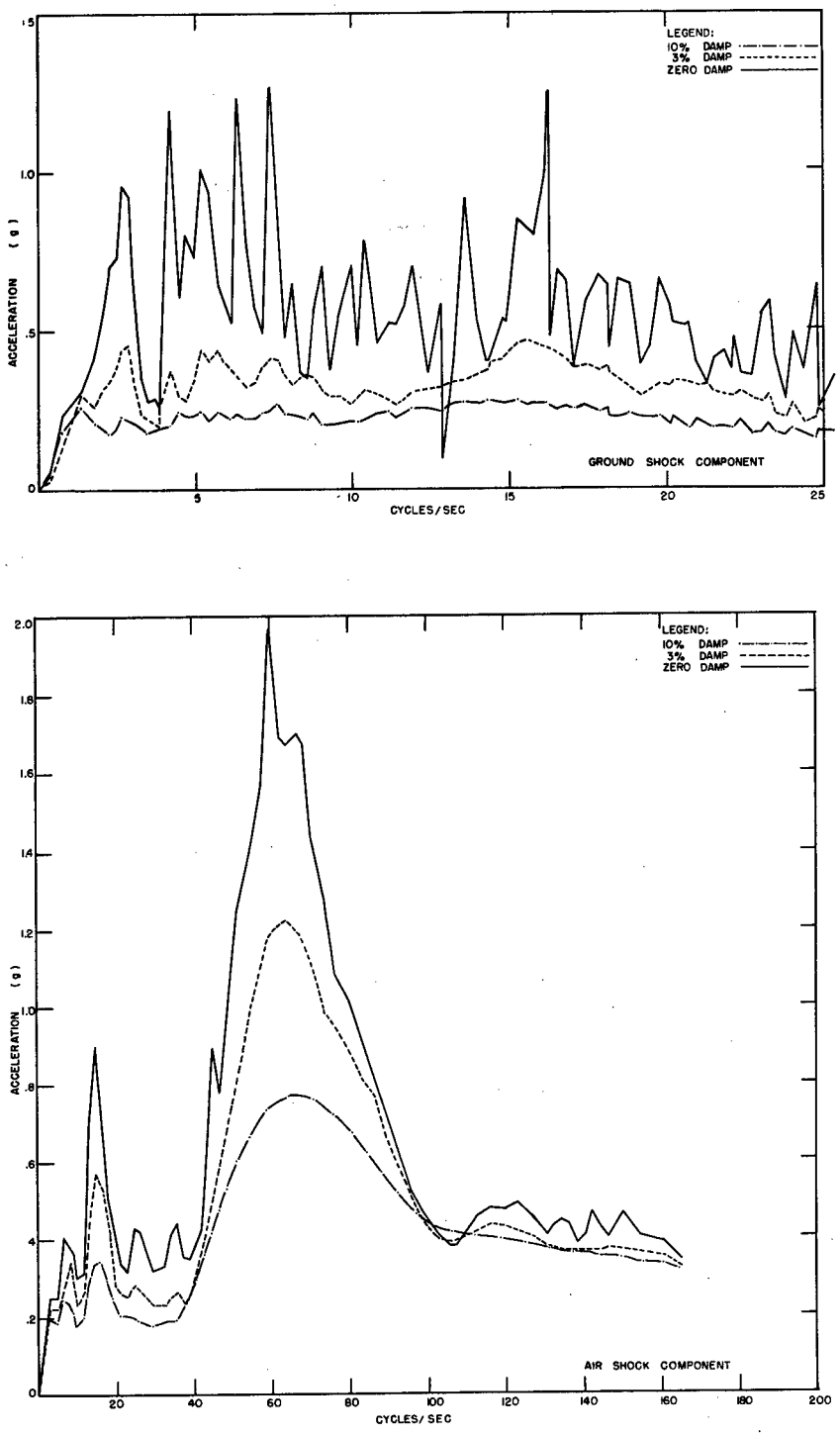

Figure A. 6 Tangential acceleration spectra, Station Kate, Operation Ivy.

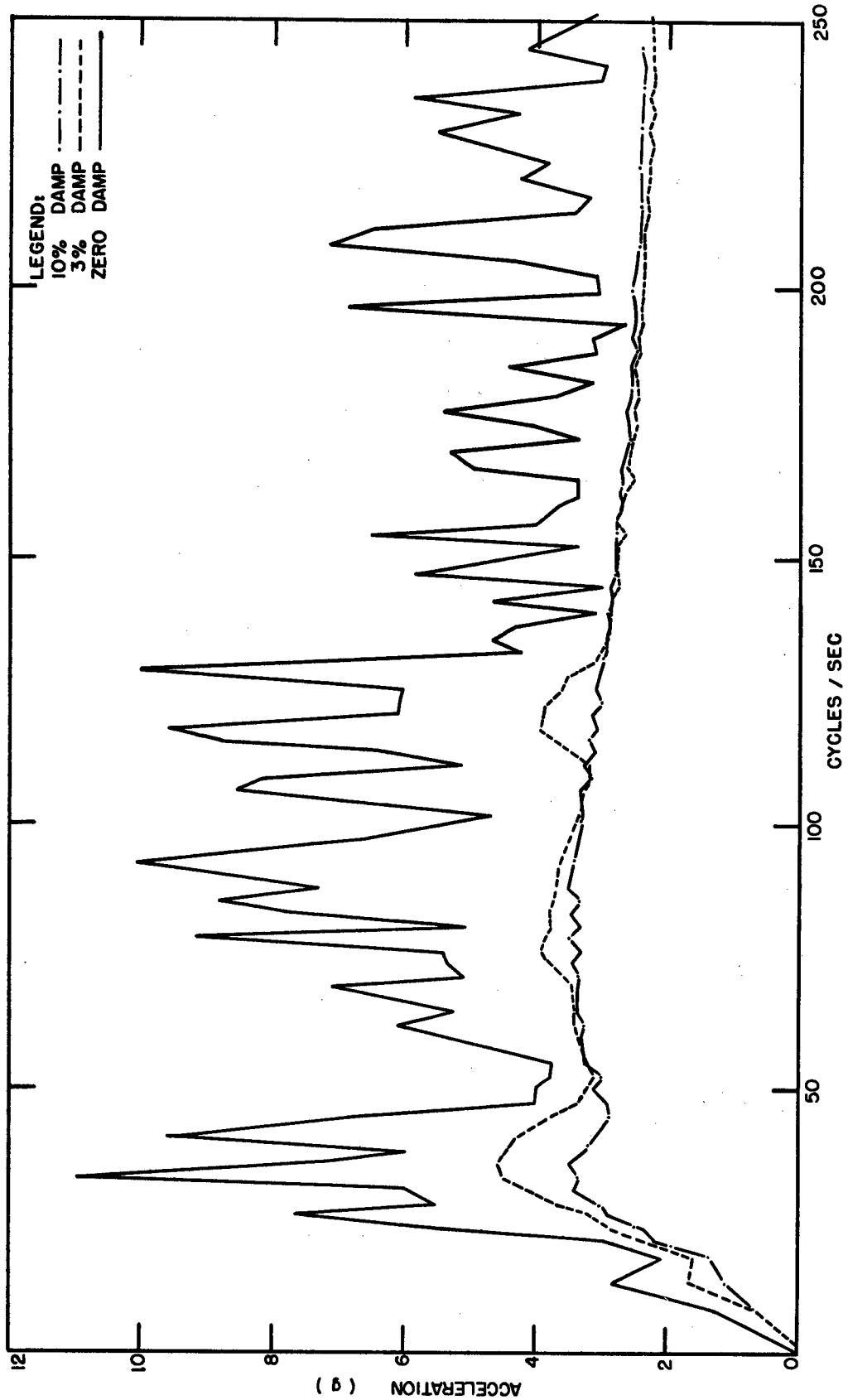

Figure A. 7 Vertical acceleration spectra, Station 3-285, Shot 1, Operation Upshot-Knothole.

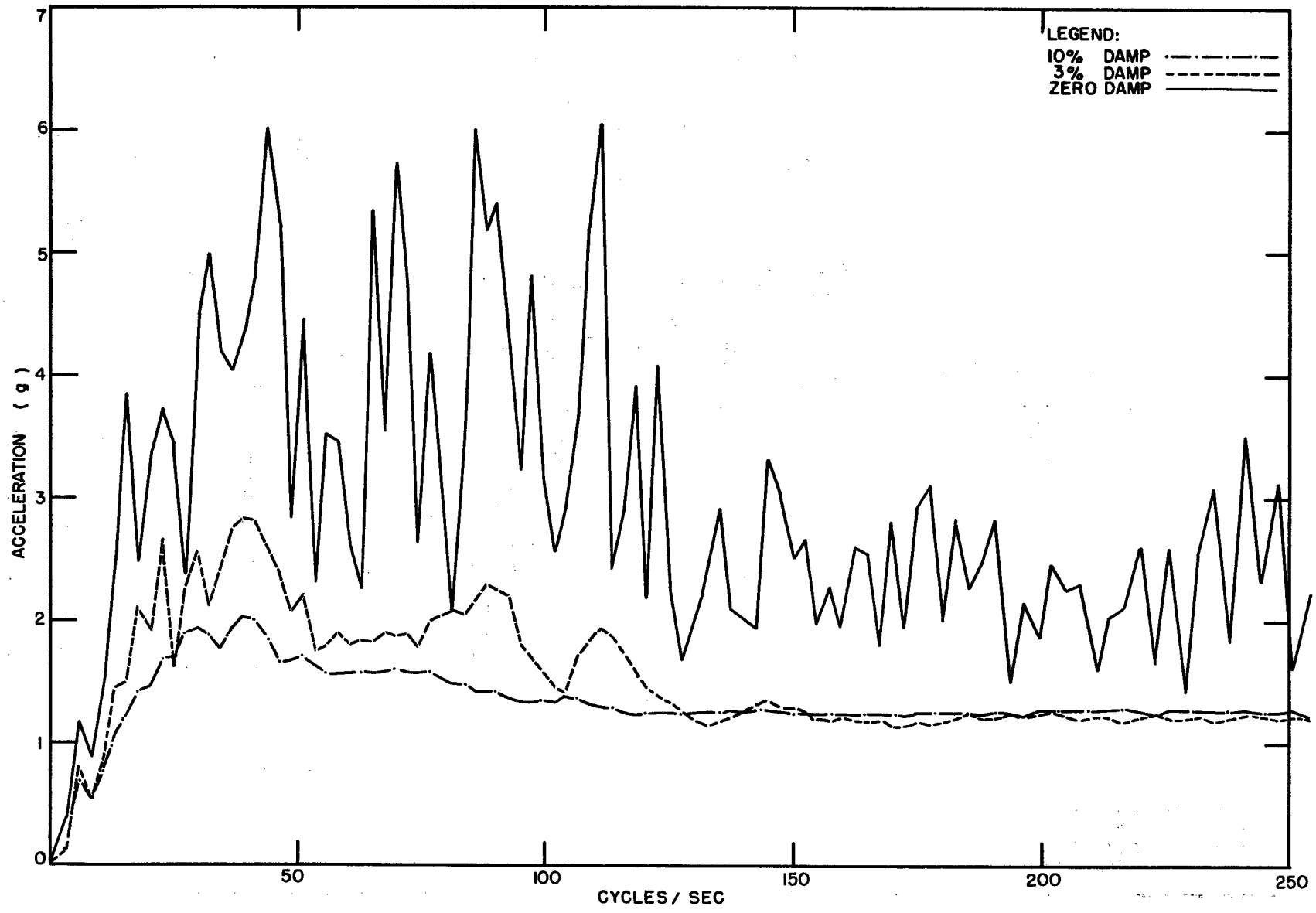

Figure A. 8 Radial acceleration spectra, Station 3-285, Shot 1, Operation Upshot-Knothole.

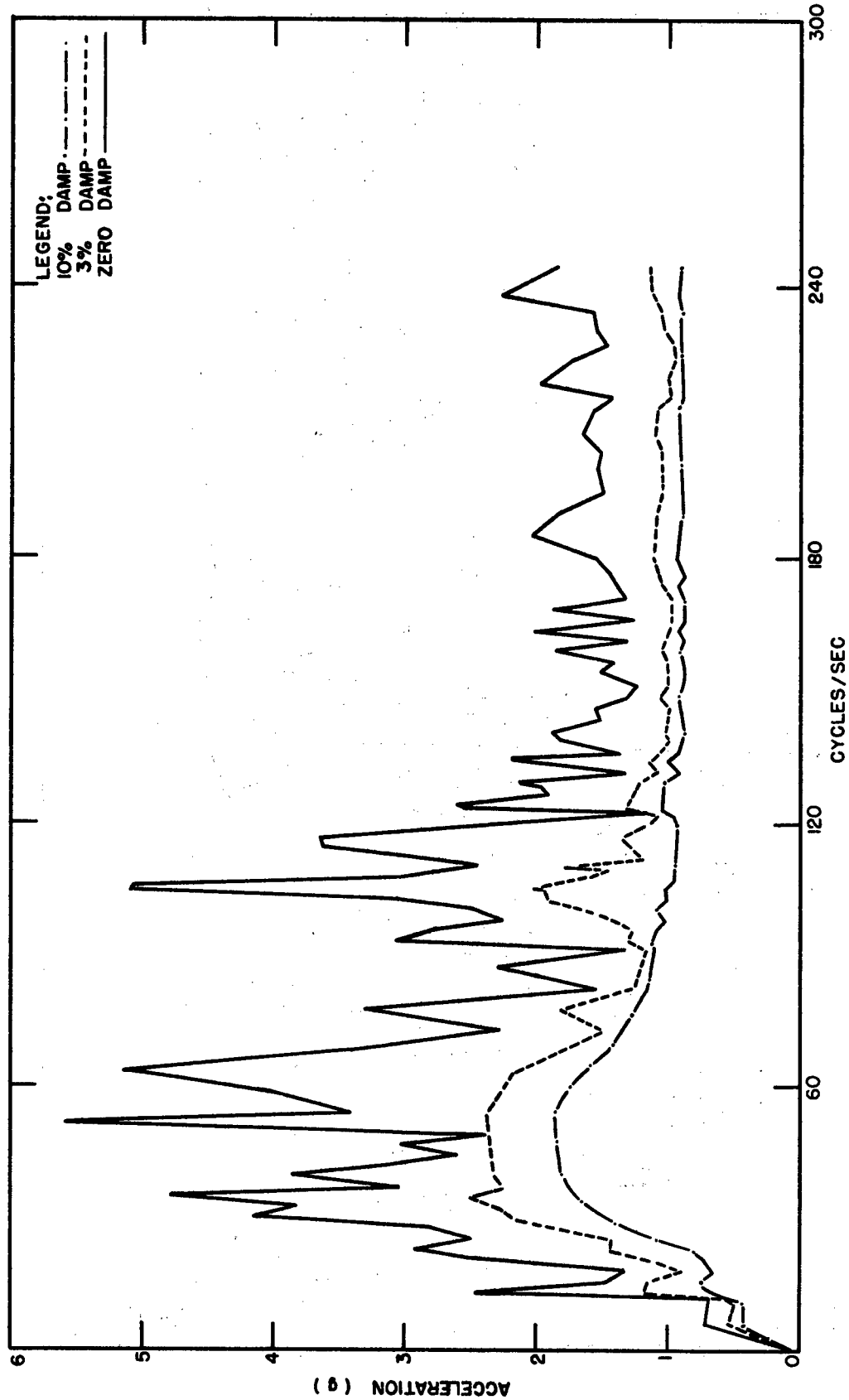

Figure A.9 Tangential acceleration spectra, Station 3-285, Shot 1, Operation Upshot-Knothole.

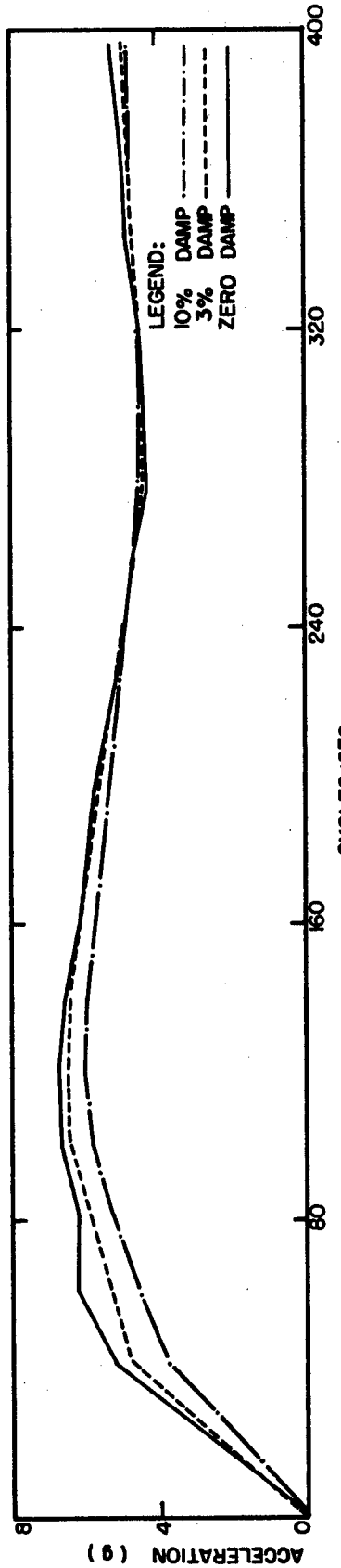

Figure A.10 Vertical acceleration spectra, Station F-281, Shot 9, Operation Upshot-Knothole.

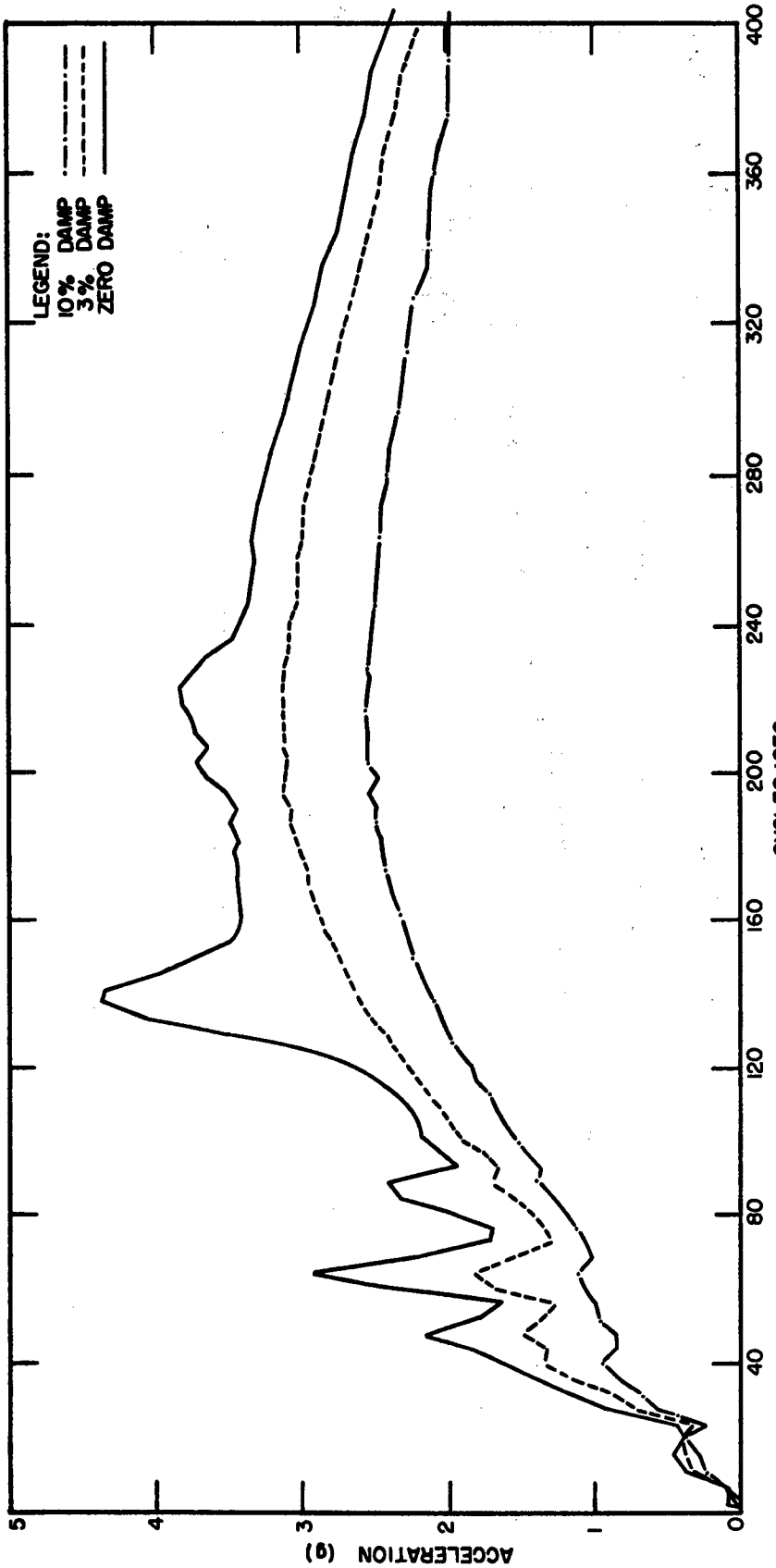

Figure A. 11 Radial acceleration spectra, Station F-281, Shot 9, Operation Upshot-Knothole.

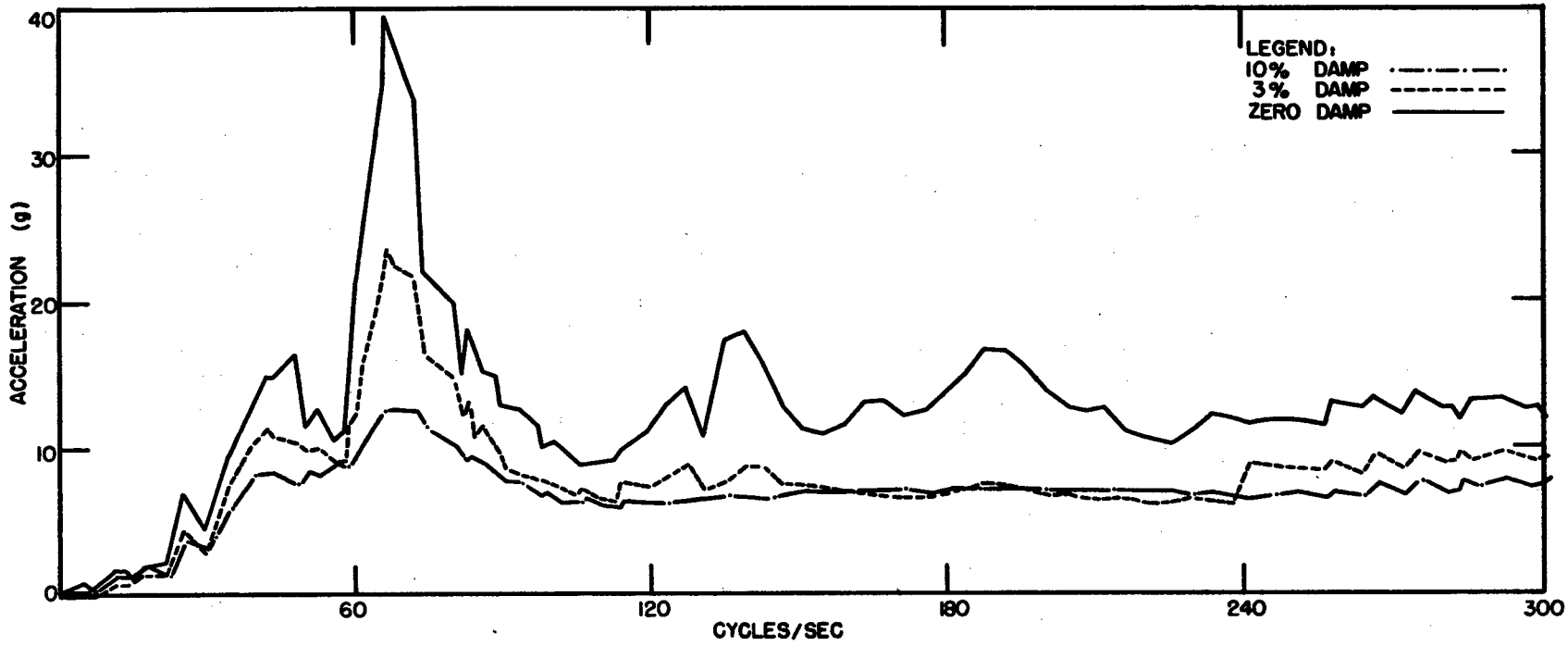

Figure A. 12 Tangential acceleration spectra, Station F-281, Shot 9, Operation Upshot-Knothole.

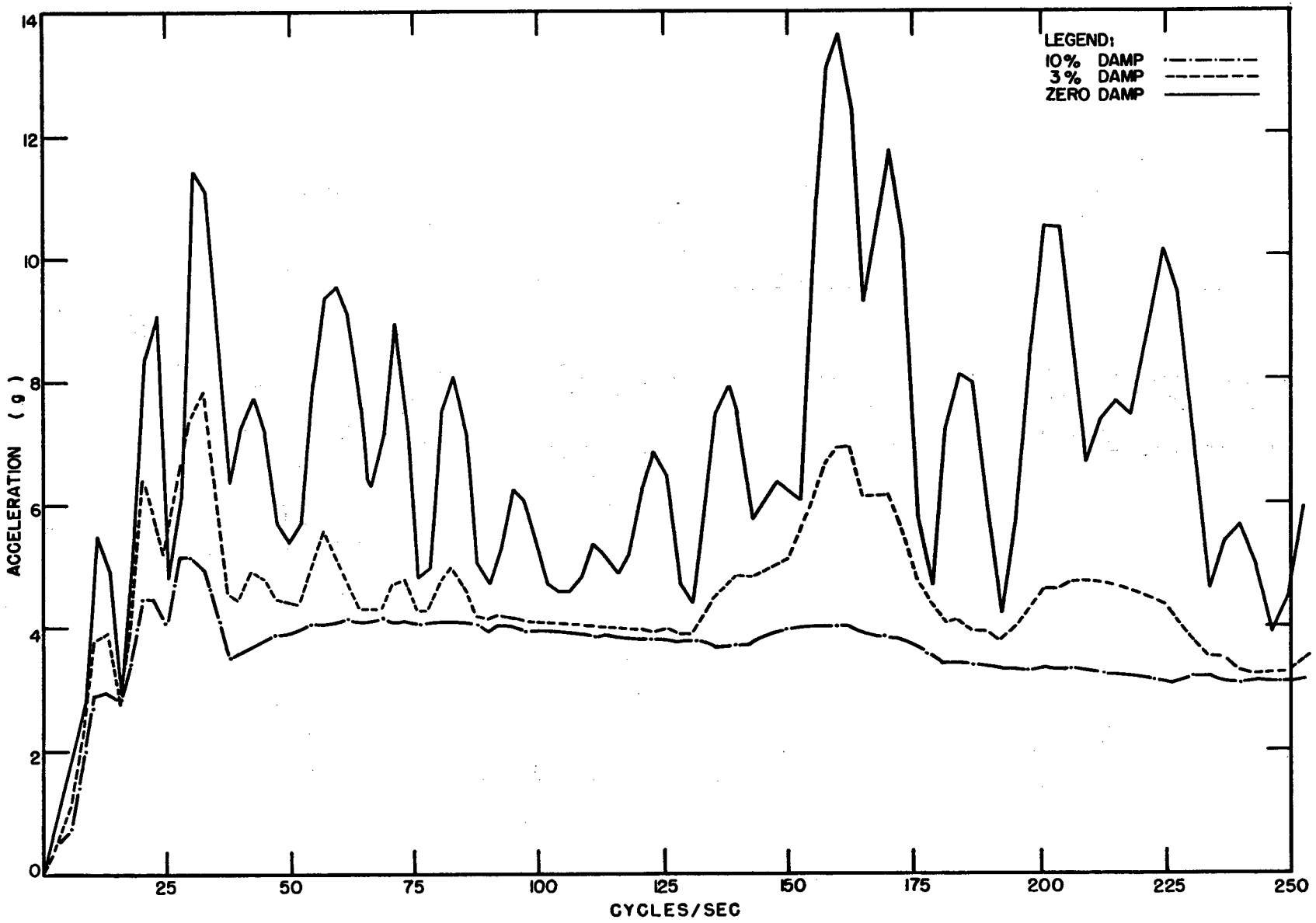

Figure A.13 Vertical acceleration spectra, Station F-281, Shot 10, Operation Upshot-Knothole.

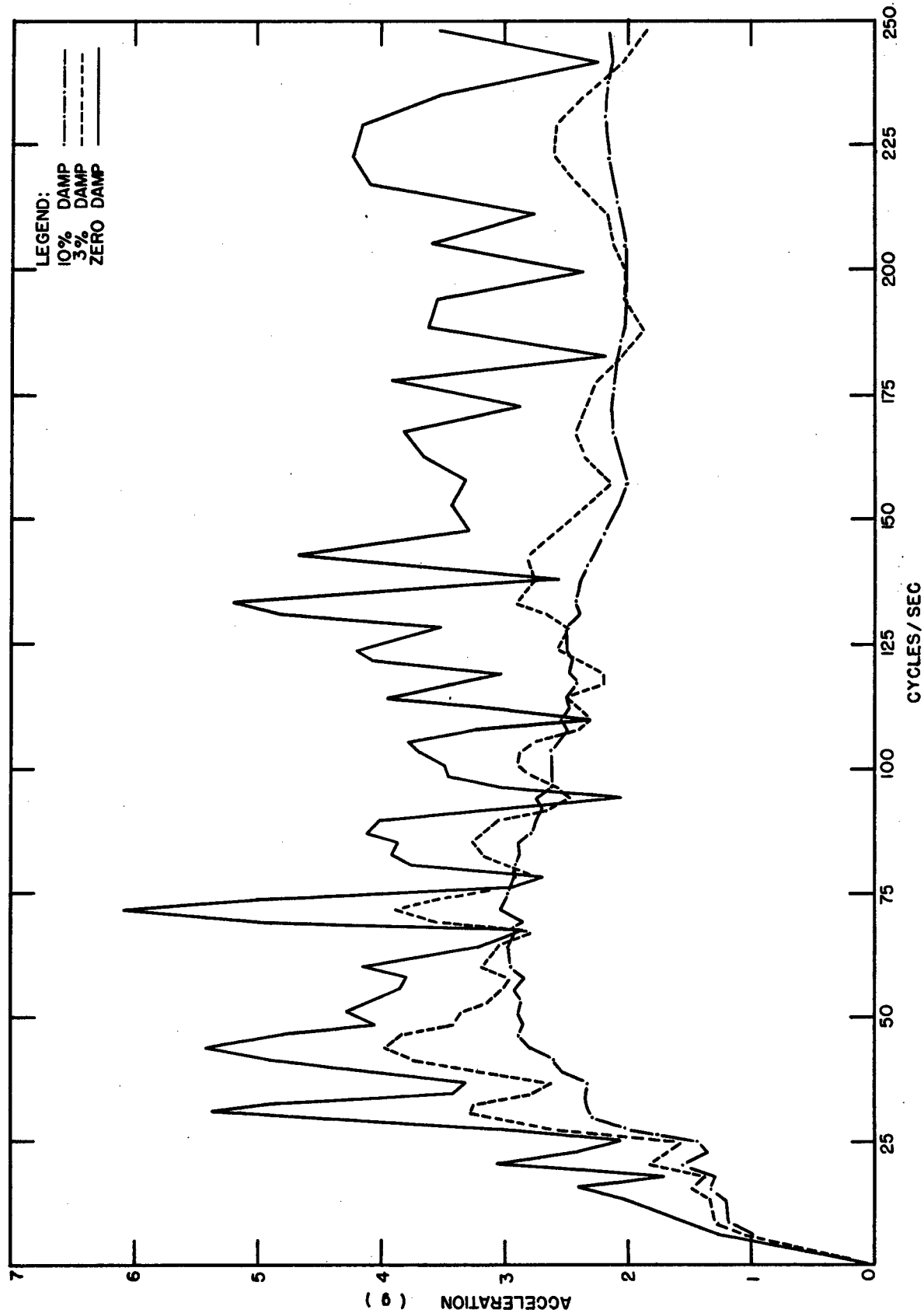

Figure A.14 Radial acceleration spectra, Station F-281, Shot 10, Operation Upshot-Knothole.

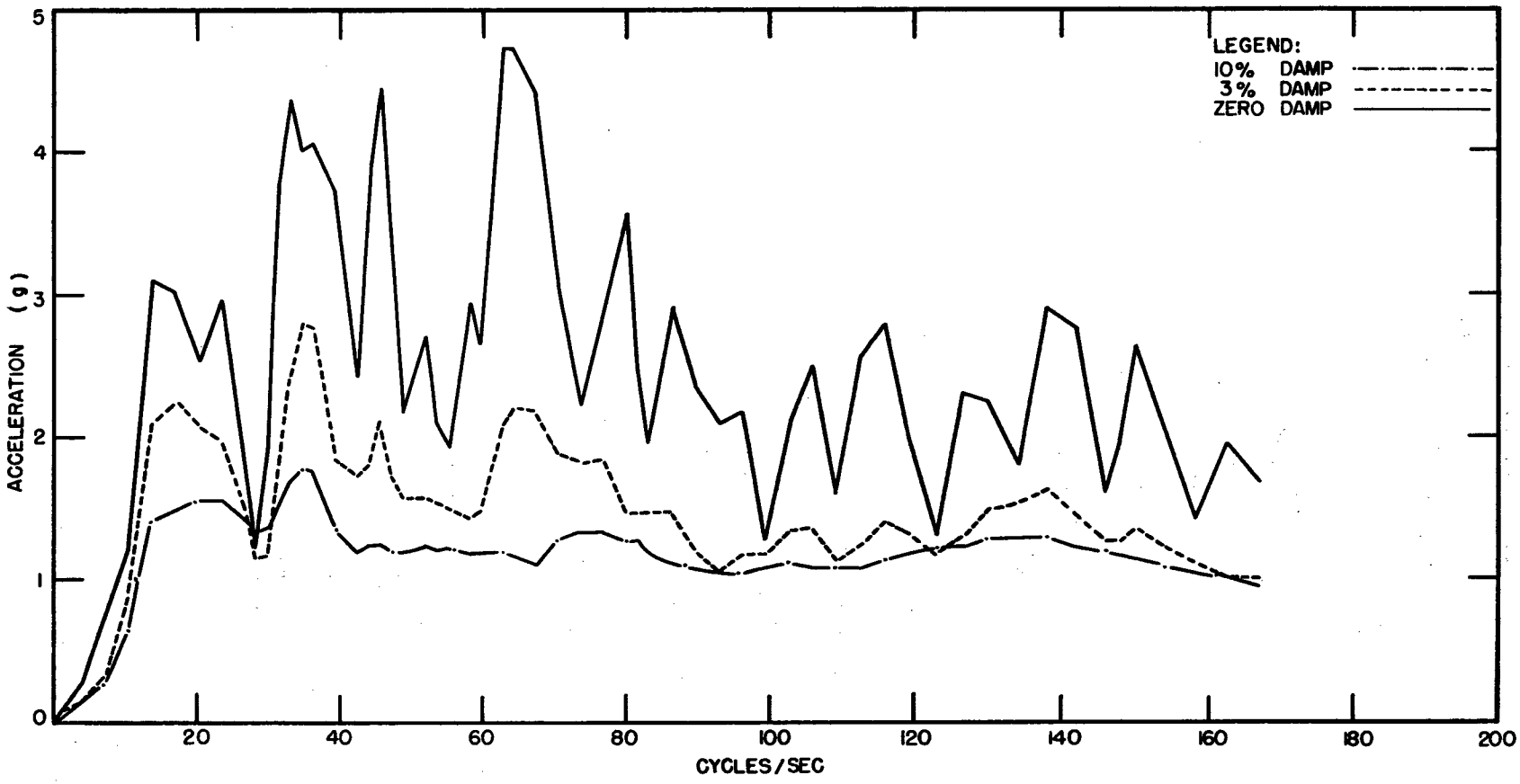

Figure A.15 Tangential acceleration spectra, Station F-281, Shot 10, Operation Upshot-Knothole.

REFERENCES

1. Perret, W. R.; Earth Stresses and Earth Strains; Operation Tumbler-Snapper, WT-503, September 1952; Sandia Corporation; CONFIDENTIAL RESTRICTED DATA.

2. Fischer, J. S., and Reisler, R. E.; Ground Acceleration Measurements; Operation TUMBLER, WT-516, January 1953; BRL/APE; SECRET RESTRICTED DATA.

3. Salmon, V., and Hornig, S. R.; Earth Acceleration vs Time and Distance; Operation TUMBLER, WT-517, February 1953; Stanford Research Institute; CONFIDENTIAL.

4. Perret, W. R., and Gentry, V. L.; Free-Field Measurements of Earth Stress, Strain, and Ground Motion; Operation UPSHOT-KNOTHOLE, WT-716, February 1955; Sandia Corporation; SECRET RESTRICTED DATA.

5. Perret, W. R.; Ground Motion Studies on Operations Ivy and Castle; WT-9002, February 1955; Sandia Corporation; SECRET RESTRICTED DATA.

DISTRIBUTION

Military Distribution Category 5-22

ARMY ACTIVITIES

1 Asst. Dep. Chief of Staff for Military Operations, D/A, Washington 25, D.C. ATTN: Asst. Executive (R&SW)
2 Chief of Research and Development, D/A, Washington 25, D.C. ATTN: Atomic Division
3 Chief of Ordnance, D/A, Washington 25, D.C. ATTN: ORDTX-AR
4 Chief Signal Officer, D/A, P&O Division, Washington 25, D.C. ATTN: SIGRD-8
5 The Surgeon General, D/A, Washington 25, D.C. ATTN: MEDNE
6- 7 Chief Chemical Officer, D/A, Washington 25, D.C.
8 The Quartermaster General, D/A, Washington 25, D.C. ATTN: Research and Development
9- 11 Chief of Engineers, D/A, Washington 25, D.C. ATTN: ENGNB
12 Chief of Transportation, Military Planning and Intelligence Div., Washington 25, D.C.
13- 15 Commanding General, Headquarters, U. S. Continental Army Command, Ft. Monroe, Va.
16 President, Board #1, Headquarters, Continental Army Command, Ft. Sill, Okla.
17 President, Board #2, Headquarters, Continental Army Command, Ft. Knox, Ky.
18 President, Board #4, Headquarters, Continental Army Command, Ft. Bliss, Tex.
19 Commanding General, U.S. Army Caribbean, Ft. Amador, C.Z. ATTN: Cml. Off.
20- 21 Commanding General, U.S. Army Europe, APO 403, New York, N.Y. ATTN: OPOT Div., Combat Dev. Br.
22- 23 Commandant, Command and General Staff College, Ft. Leavenworth, Kan. ATTN: AILLS(AS)
24 Commandant, The Artillery and Missile School, Ft. Sill, Okla.
25 Secretary, The U.S. Army Air Defense School, Ft. Bliss, Texas. ATTN: Maj. Gregg D. Breitegan, Dept. of Tactics and Combined Arms
26 Commanding General, Army Medical Service School, Brooke Army Medical Center, Ft. Sam Houston, Tex.
27 Director, Special Weapons Development Office, Headquarters, CONARC, Ft. Bliss, Tex. ATTN: Capt. T. E. Skinner
28 Commandant, Walter Reed Army Institute of Research, Walter Reed Army Medical Center, Washington 25, D. C.
29 Superintendent, U.S. Military Academy, West Point, N. Y. ATTN: Prof. of Ordnance
30 Commandant, Chemical Corps School, Chemical Corps Training Command, Ft. McClellan, Ala.
31 Commanding General, U.S. Army Chemical Corps, Research and Development Command, Washington, D.C.
32- 33 Commanding General, Aberdeen Proving Grounds, Md. ATTN: Director, Ballistics Research Laboratory
34 Commanding General, The Engineer Center, Ft. Belvoir, Va. ATTN: Asst. Commandant, Engineer School
35 Commanding Officer, Engineer Research and Development Laboratory, Ft. Belvoir, Va. ATTN: Chief, Technical Intelligence Branch
36 Commanding Officer, Picatinny Arsenal, Dover, N.J. ATTN: ORDBB-TK
37 Commanding Officer, Army Medical Research Laboratory, Ft. Knox, Ky.
38- 39 Commanding Officer, Chemical Warfare Laboratories, Army Chemical Center, Md. ATTN: Tech. Library
40 Commanding Officer, Transportation R&D Station, Ft. Eustis, Va.
41 Director, Technical Documents Center, Evans Signal Laboratory, Belmar, N.J.
42 Director, Waterways Experiment Station, PO Box 631, Vicksburg, Miss. ATTN: Library
43 Director, Armed Forces Institute of Pathology, Walter Reed Army Medical Center, 6825 16th Street, N.W., Washington 25, D.C.
44 Operations Research Office, Johns Hopkins University, 6935 Arlington Rd., Bethesda 14, Md.
45- 46 Commanding General, Quartermaster Research and Development, Command, Quartermaster Research and Development Center, Natick, Mass. ATTN: CBR Liaison Officer
47 Commanding Officer, Diamond Ordnance Fuze Laboratories, Washington 25, D.C. ATTN: Coordinator, Atomic Weapons Effects Tests
48 Commanding General, Quartermaster Research and Engineering Command, U.S. Army, Natick, Mass.
49- 54 Technical Information Service Extension, Oak Ridge, Tenn.

NAVY ACTIVITIES

55- 56 Chief of Naval Operations, D/N, Washington 25, D. C. ATTN: OP-36
57 Chief of Naval Operations, D/N, Washington 25, D.C. ATTN: OP-03EG
58 Chief, Bureau of Medicine and Surgery, D/N, Washington 25, D.C. ATTN: Special Weapons Defense Div.
59 Chief, Bureau of Ordnance, D/N, Washington 25, D.C.
60 Chief, Bureau of Ships, D/N, Washington 25, D.C. ATTN: Code 348
61 Chief, Bureau of Yards and Docks, D/N, Washington 25, D.C. ATTN: D-440
62 Chief, Bureau of Supplies and Accounts, D/N, Washington 25, D.C.
63- 64 Chief, Bureau of Aeronautics, D/N, Washington 25, D.C.
65 Chief of Naval Research, Department of the Navy Washington 25, D.C. ATTN: Code 811
66 Commander-in-Chief, U.S. Atlantic Fleet, U.S. Naval Base, Norfolk 11, Va.
67- 70 Commandant, U.S. Marine Corps, Washington 25, D.C. ATTN: Code A03H
71 President, U.S. Naval War College, Newport, R.I.
72 Superintendent, U.S. Naval Postgraduate School, Monterey, Calif.
73 Commanding Officer, U.S. Naval Schools Command, U.S. Naval Station, Treasure Island, San Francisco, Calif.
74 Commanding Officer, U.S. Fleet Training Center, Naval Base, Norfolk 11, Va. ATTN: Special Weapons School
75- 76 Commanding Officer, U.S. Fleet Training Center, Naval Station, San Diego 36, Calif. ATTN: (SPWP School)
77 Commanding Officer, U.S. Naval Damage Control Training Center, Naval Base, Philadelphia, Pa. ATTN: ABC Defense Course
78 Commander, U.S. Naval Ordnance Laboratory, Silver Spring 19, Md. ATTN: EE
79 Commander, U.S. Naval Ordnance Laboratory, Silver Spring 19, Md. ATTN: R
80 Commander, U.S. Naval Ordnance Test Station, Inyokern, China Lake, Calif.
81 Officer-in-Charge, U.S. Naval Civil Engineering Res. and Evaluation Lab., U.S. Naval Construction Battalion Center, Port Hueneme, Calif. ATTN: Code 753
82 Commanding Officer, U.S. Naval Medical Research Inst., National Naval Medical Center, Bethesda 14, Md.
83 Director, Naval Air Experimental Station, Air Material Center, U.S. Naval Base, Philadelphia, Penn.
84 Director, U.S. Naval Research Laboratory, Washington 25, D.C. ATTN: Mrs. Katherine H. Cass

85 Commanding Officer and Director, U.S. Navy Electronics Laboratory, San Diego 52, Calif. ATTN: Code 4223
86- 87 Commanding Officer, U.S. Naval Radiological Defense Laboratory, San Francisco, Calif. ATTN: Technical Information Division
88- 89 Commanding Officer and Director, David W. Taylor Model Basin, Washington 7, D.C. ATTN: Library
90 Commander, U.S. Naval Air Development Center, Johnsville, Pa.
91 Commanding Officer and Director, U.S. Naval Engineering Experiment Station, Annapolis, Md. ATTN: Code 155
92 Commander-in-Chief Pacific, Pearl Harbor, TH
93 Commander, Norfolk Naval Shipyard, Portsmouth 8, Va. ATTN: Code 270
94- 97 Technical Information Service Extension, Oak Ridge, Tenn. (Surplus)

AIR FORCE ACTIVITIES

98 Asst. for Atomic Energy Headquarters, USAF, Washington 25, D.C. ATTN: DCS/O
99 Director of Operations, Headquarters, USAF, Washington 25, D.C. ATTN: Operations Analysis
100 Director of Plans, Headquarters, USAF, Washington 25, D.C. ATTN: War Plans Div.
101 Director of Research and Development, DCS/D, Headquarters, USAF, Washington 25, D.C. ATTN: Combat Components Div.
102-103 Director of Intelligence, Headquarters, USAF, Washington 25, D.C. ATTN: AFOIN-IB2
104 The Surgeon General, Headquarters, USAF, Washington 25, D.C. ATTN: Bio. Def. Br., Pre. Med. Div.
105 Asst. Chief of Staff, Intelligence, Headquarters, U.S. Air Forces-Europe, APO 633, New York, N.Y. ATTN: Directorate of Air Targets
106 Commander, 497th Reconnaissance Technical Squadron (Augmented), APO 633, New York, N.Y.
107 Commander, Far East Air Forces, APO 925, San Francisco, Calif. ATTN: Special Asst. for Damage Control
108 Commander-in-Chief, Strategic Air Command, Offutt Air Force Base, Omaha, Nebraska. ATTN: OAWS
109 Commander, Tactical Air Command, Langley AFB, Va. ATTN: Documents Security Branch
110 Commander, Air Defense Command, Ent AFB, Colo.
111-112 Research Directorate, Headquarters, Air Force Special Weapons Center, Kirtland Air Force Base, New Mexico, ATTN: Blast Effects Res.
113-115 Assistant for Operations Analysis, DCS/Operations, ATTN: Missile Survival Study Group (Mr. Tuttle), Headquarters, USAF, Washington 25, D.C.
116 Director of Installations, DCS/O, Headquarters, USAF, Washington 25, D.C. ATTN: AFOIE-E
117 Commander, Air Research and Development Command, Andrews AFB, Washington 25, D.C. ATTN: RDDN
118 Commander, Air Proving Ground Command, Eglin AFB, Fla. ATTN: Adj./Tech. Report Branch
119-120 Director, Air University Library, Maxwell AFB, Ala.
121-128 Commander, Flying Training Air Force, Waco, Tex. ATTN: Director of Observer Training
129 Commander, Crew Training Air Force, Randolph Field, Tex. ATTN: 2GTS, DCS/O
130-131 Commandant, Air Force School of Aviation Medicine, Randolph AFB, Tex.
132-137 Commander, Wright Air Development Center, Wright-Patterson AFB, Dayton, O. ATTN: WCOSI
138-139 Commander, Air Force Cambridge Research Center, LG Hanscom Field, Bedford, Mass. ATTN: CRQST-2
140-142 Commander, Air Force Special Weapons Center, Kirtland AFB, N. Mex. ATTN: Library
143 Commander, Lowry AFB, Denver, Colo. ATTN: Department of Special Weapons Training
144 Commander, 1009th Special Weapons Squadron, Headquarters, USAF, Washington 25, D.C.
145-146 The RAND Corporation, 1700 Main Street, Santa Monica, Calif. ATTN: Nuclear Energy Division
147 Commander, Second Air Force, Barksdale AFB, Louisiana. ATTN: Operations Analysis Office
148 Commander, Eighth Air Force, Westover AFB, Mass. ATTN: Operations Analysis Office
149 Commander, Fifteenth Air Force, March AFB, Calif. ATTN: Operations Analysis Office
150 Commander, Western Development Div. (ARDC), PO Box 262, Inglewood, Calif. ATTN: WDSIT, Mr. R. G. Weitz
151-155 Technical Information Service Extension, Oak Ridge, Tenn. (Surplus)

OTHER DEPARTMENT OF DEFENSE ACTIVITIES

156 Asst. Secretary of Defense, Research and Engineering, D/D, Washington 25, D.C. ATTN: Tech. Library
157 U.S. Documents Officer, Office of the U.S. National Military Representative, SHAPE, APO 55, New York, N.Y.
158 Director, Weapons Systems Evaluation Group, OSD, Rm 2E1006, Pentagon, Washington 25, D.C.
159 Chairman, Armed Services Explosives Safety Board, D/D, Building T-7, Gravelly Point, Washington 25, D.C.
160 Commandant, Armed Forces Staff College, Norfolk 11, Va. ATTN: Secretary
161 Commander, Field Command, Armed Forces Special Weapons Project, PO Box 5100, Albuquerque, N. Mex.
162 Commander, Field Command, Armed Forces Special Weapons Project, PO Box 5100, Albuquerque, N. Mex. ATTN: Technical Training Group
163-164 Commander, Field Command, Armed Forces Special Weapons Project, P.O. Box 5100, Albuquerque, N. Mex. ATTN: Deputy Chief of Staff, Weapons Effects Test
165-175 Chief, Armed Forces Special Weapons Project, Washington 25, D.C. ATTN: Documents Library Branch
176-180 Technical Information Service Extension, Oak Ridge, Tenn. (Surplus)

ATOMIC ENERGY COMMISSION ACTIVITIES

181-183 U.S. Atomic Energy Commission, Classified Technical Library, Washington 25, D.C. ATTN: Mrs. J. M. O'Leary (For DMA)
184-185 Los Alamos Scientific Laboratory, Report Library, PO Box 1663, Los Alamos, N. Mex. ATTN: Helen Redman
186-200 Sandia Corporation, Classified Document Division, Sandia Base, Albuquerque, N. Mex. ATTN: H. J. Smyth, Jr.
201-203 University of California Radiation Laboratory, PO Box 808, Livermore, Calif. ATTN: Clovis G. Craig
204 Weapon Data Section, Technical Information Service Extension, Oak Ridge, Tenn.
205-225 Technical Information Service Extension, Oak Ridge, Tenn. (Surplus)